Title

Functional and Representational Differences Between the Bilateral Inferior Temporal Numeral Areas

Authors

Darren J. Yeo [a, b], Courtney Pollack [a], Benjamin N. Conrad [a], Gavin R. Price [a, c, †, *]

Author Affiliations

[a] Department of Psychology & Human Development, Peabody College, Vanderbilt University, 230 Appleton Place, Nashville, TN, 37203

[b] Division of Psychology, School of Social Sciences, Nanyang Technological University, 48 Nanyang Avenue, Singapore, 639818

[c] Department of Psychology, University of Exeter, Washington Singer Building Perry Road, Exeter, EX4 4QG, United Kingdom

[*] **Corresponding Author:**

Gavin R. Price

Email: g.r.price@exeter.ac.uk

Department of Psychology, University of Exeter, Washington Singer Building Perry Road, Exeter, EX4 4QG, United Kingdom

[†]This work was completed while Gavin R. Price was employed at Vanderbilt University

Note: This work was prepared while Courtney Pollack was employed at Vanderbilt University. The opinions expressed in this article are the author's own and do not reflect the view of the National Institutes of Health, the Department of Health and Human Services, or the United States government.

Abstract

The processing of numerals as visual objects is supported by an "Inferior Temporal Numeral Area" (ITNA) in the bilateral inferior temporal gyri (ITG). Extant findings suggest some degree of hemispheric asymmetry in how the bilateral ITNAs process numerals. Pollack and Price (2019) reported such a hemispheric asymmetry by which a region in the left ITG was sensitive to digits during a visual search for a digit among letters, and a homologous region in the right ITG that showed greater digit sensitivity in individuals with higher calculation skills. However, the ITG regions were localized with separate analyses without directly contrasting their digit sensitivities and relation to calculation skills. So, the extent of and reasons for these functional asymmetries remain unclear. Here we probe whether the functional and representational properties of the ITNAs are asymmetric by applying both univariate and multivariate region-of-interest analyses to Pollack and Price's (2019) data. Contrary to the implications of the original findings, digit sensitivity did not differ between ITNAs, and digit sensitivity in both left and right ITNAs was associated with calculation skills. Representational similarity analyses revealed that the overall representational geometries of digits in the ITNAs were also correlated, albeit weakly, but the representational contents of the ITNAs were largely inconclusive. Nonetheless, we found a right lateralization in engagement in alphanumeric categorization, and that the right ITNA showed greater discriminability between digits and letters. Greater right lateralization of digit sensitivity and digit discriminability in the left ITNA were also related to higher calculation skills. Our findings thus suggest that the ITNAs may not be functionally identical and should be directly contrasted in future work. Our study also highlights the importance of within-individual comparisons for understanding hemispheric asymmetries, and analyses of individual differences and multivariate features to uncover effects that would otherwise be obscured by averages.

Keywords: hemispheric asymmetry; number form area; numerical cognition; object categorization

Introduction

Regardless of the writing scripts our native languages adopt, almost everyone has to master the Arabic numeral system, comprising the digits 0 – 9, to function successfully in modern societies. As the foundational years of formal education typically have separate numeracy and literacy classes, the learning of Arabic numerals and native language writing systems tends to be highly contextualized. The repeated and predictable use of Arabic numerals mostly in numeracy contexts may influence how our brains are organized to identify and distinguish Arabic numerals from other character categories (Gauthier, 2000; see Hannagan et al., 2015, for a review; Yeo et al., 2020).

An emerging body of work using functional magnetic resonance imaging (fMRI), and intracranial recording and stimulation has shown a consistent location in the right posterior inferior temporal gyrus (ITG) (MNI[1] 55, -50, -12; see Yeo et al., 2017, for a meta-analysis) and/or its left homolog that works with other cortical regions to support the processing of Arabic numerals (Amalric & Dehaene, 2016; Grotheer et al., 2018; Grotheer, Herrmann, et al., 2016; Pollack & Price, 2019; Roux et al., 2008; Shum et al., 2013). It is usually identified as a region in the occipitotemporal cortex that exhibits greater sensitivity in terms of response amplitude to Arabic numerals than to other stimuli such as letters and novel characters. Hereafter, we will refer to such a ventral occipitotemporal (vOT) node of the neural circuit underlying numeral identification as the "Inferior Temporal Numeral Area" (ITNA). This label follows the naming convention of other category-selective regions in specifying its anatomical location and its category preference (Grill-Spector & Weiner, 2014; Grotheer et al., 2018) without presupposing the features of a stimulus it represents (e.g., shape as presumed in its former label "Number Form Area") (Yeo et al., 2020). The ITNA label is also useful for distinguishing it from an adjacent neuronal population that is not selective for

[1] Using the tal2icbm_spm.m transform (brainmap.org/icbm2tal) (Lancaster et al., 2007).

Arabic numerals, but to any stimuli used in mathematical manipulation, such as arithmetic (Daitch et al., 2016; Grotheer et al., 2018; Pinheiro-Chagas et al., 2018). Last but not least, labeling the ITG node as ITNA does not imply that it functions in isolation, but in interactive loops with other regions in the parietal and frontal associative cortices (Baek et al., 2018; Daitch et al., 2016).

Although evidence from split-brain patients suggests that the visual systems in both hemispheres are capable of recognizing and processing single Arabic digits (Cohen & Dehaene, 1996; Colvin et al., 2005; see Dehaene & Cohen, 1995, for a review; Sergent, 1990; Seymour et al., 1994; Teng & Sperry, 1973), studies that employed a variety of numerical tasks including multi-digit numeral naming, same-different judgment, magnitude comparison, and arithmetic in patients with left vOT lesions (Cohen & Dehaene, 1991, 1995, 2000; Miozzo & Caramazza, 1998) or split brains (Cohen & Dehaene, 1996; Gazzaniga & Smylie, 1984; Seymour et al., 1994) suggest that the left and right ITNAs (and the circuits they are a part of) are neither a single functional unit, nor functional duplicates working in parallel, but are functionally dissimilar and independent depending on the task contexts. Moreover, cerebral hemispheres are more efficient in identifying alphanumeric characters independently in isolation than when they had to communicate with each other (Teng & Sperry, 1973), which suggests stronger intra-hemispheric interactions than inter-hemispheric interactions. Such neuropsychological evidence led Cohen and Dehaene (1995) to propose that we possess "two number identification systems, possibly residing in different hemispheres, and which may be separately called upon depending on the task" (p. 123).

According to the "Triple-code Model" of number processing (Dehaene, 1992; Dehaene & Cohen, 1995), numbers can be represented mentally and neurally via three distinct codes: (1) a *visual number form* code, in which numbers are represented as a structured array of Arabic digits; (2) a *magnitude* code, in which numbers are represented semantically as distributions of activation on a

mental number line (Dehaene & Changeux, 1993; Verguts & Fias, 2004); and (3) a *verbal word frame* code, in which numbers are represented asemantically as a sequence of words. The left hemispheric number identification system is hypothesized to be necessary for tasks that rely on verbal processes (e.g., reading aloud multi-digit numerals and retrieval of verbally encoded arithmetic facts) due to its co-lateralization with the left-lateralized language system (Cohen & Dehaene, 1995; Dehaene & Cohen, 1997; Pinel & Dehaene, 2010) (see Figure 1). Regions involved in the visual number form code were originally referred to as "visual number form" areas (Grotheer, Herrmann, et al., 2016; Shum et al., 2013), following the naming of its better-known word-selective counterpart, the "visual word form area" (Dehaene & Cohen, 2011).

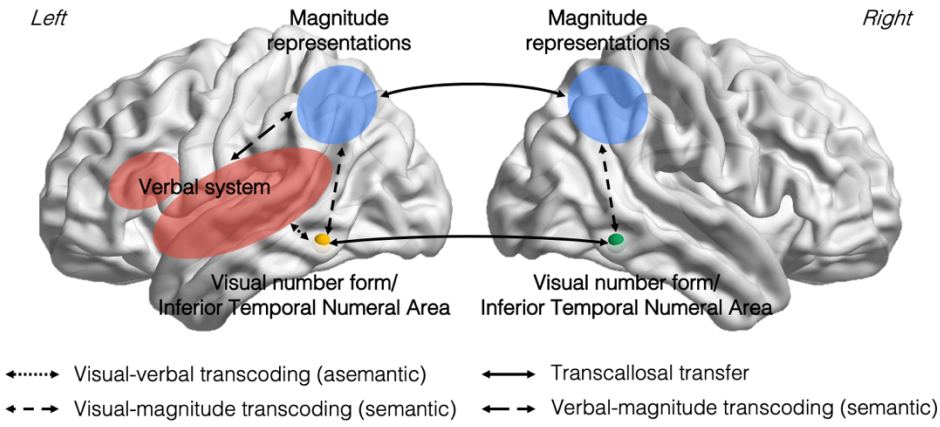

Figure 1. A schematic of the functional and anatomical assumptions of the Triple-code Model adapted from Dehaene & Cohen (1995).

Although there is now a significant body of evidence supporting the existence of bilateral ITNAs in adults, a non-systematic and non-exhaustive review in Table 1 shows that lateralization of numeral processing is not uncommon. In fact, a recent meta-analysis of fMRI studies that contrasted Arabic numerals to other familiar symbol categories revealed a convergence only in a right ITNA

(Yeo et al., 2017). One possibility for the lack of meta-analytic convergence in a left ITNA could be due to greater variability in its location, possibly resulting from competition for neuronal space by spatially varied left-lateralized letter- and word-preferring regions (Glezer & Riesenhuber, 2013). Another possibility is that varied task demands involving the left-hemispheric language system may recruit a left ITNA to different extents across studies.

Table 1
Evidence of lateralization of numeral processing in the ventral occipitotemporal (vOT) in adult fMRI, EEG and MEG studies

Left lateralization	Right lateralization	Bilateral
Fernandes et al. (2005): fMRI	Pinel et al. (1999): fMRI	Dehaene (1996): EEG
Fias et al. (2007): fMRI	Pinel et al. (2001): fMRI	Basso et al. (2003): fMRI
Holloway et al. (2013): fMRI	Knops et al. (2006): fMRI	Amalric & Dehaene (2016): fMRI
Vogel et al. (2015): fMRI	Gullick & Temple (2011): fMRI	Grotheer et al. (2016): fMRI
Vogel et al. (2017): fMRI	Park et al. (2012): fMRI	Grotheer et al. (2018): fMRI
Pollack & Price (2019): fMRI	Cui et al. (2013): fMRI	Bugden et al. (2019): fMRI
	Park et al. (2014): EEG	Aurtenetxe et al. (2020): MEG
	Abboud et al. (2015): fMRI	
	Carreiras, Monahan, et al. (2015): MEG	
	Carreiras, Quiñones, et al. (2015): fMRI	
	Cummine et al. (2015): fMRI	
	Park et al. (2018): EEG	
	Lochy & Schiltz (2019): EEG	
	Goffin, Sokolowski, et al. (2019): fMRI	
	Goffin, Vogel, et al. (2019): fMRI	
	Conrad et al. (2020): fMRI	

Note. EEG: electrical encephalography. MEG: magnetic encephalography. fMRI: functional magnetic resonance imaging. For EEG and MEG, vOT involvement is typically characterized by event-related potentials within the first 200 milliseconds of stimulus onset (e.g., N170 component) or by frequency tagging. Intracranial recording studies were excluded as the constraint of electrode placements precluded any inference that could be made regarding lateralization.

Among the fMRI studies that observed a bilateral engagement of the numeral identification systems in Table 1, some found no hemispheric differences in the activation profiles of the bilateral ITNAs to a diverse range of object and written character categories (Grotheer et al., 2018; Grotheer, Herrmann, et al., 2016), while others do report evidence of hemispheric asymmetry in certain

functional properties of the bilateral ITNAs (Amalric & Dehaene, 2016; Pollack & Price, 2019). In a study by Amalric and Dehaene (2016), the authors examined the response profile of each ITNA using separate group-level region-of-interest analyses. Compared to non-mathematicians, professional mathematicians had an enhanced sensitivity to well-known mathematical constants in Arabic numeral format (e.g., 3.14159 [π]) relative to non-symbolic object categories in the left ITNA, but not in the right ITNA (Amalric & Dehaene, 2016). Mathematicians also had an enhanced sensitivity to mathematical formulas in the bilateral ITNAs (Amalric & Dehaene, 2016). Although the authors did not speculate how mathematical expertise defined categorically might underlie the left lateralization, it is possible that the frequent use of those well-known mathematical constants and formulas could have led to their lexicalization in mathematicians. Such lexicalization may rely on a left-lateralized verbal pathway. It is not clear, however, whether hemispheric asymmetry exists in non-mathematicians, although a trend for greater sensitivity and selectivity to Arabic numerals in the right ITNA relative to the left ITNA was observed (see Figure 8E in Amalric & Dehaene, 2016).

Recently, an intriguing hemispheric asymmetry in the bilateral ITNAs was observed in a study by Pollack and Price (2019). In that study, adults performed a visual search task in which they had to detect whether a digit was present among a string of letters (e.g., 'T S N 2 R') or not (e.g., 'A H T N R'). In a whole-brain localization analysis, they found that a region in the left (but not the right) ITG (MNI -57, -52, -11) was more engaged when a digit was present than when a digit was absent (i.e., [Digit Present > Digit Absent]; hereafter, we refer to this differential response as "digit sensitivity") (Figure 2a). A brain-behavior correlational analysis revealed a homologous region in the right ITG (but not the left) (MNI 54, -52, -14) in which individuals with higher symbolic calculation skills showed greater digit sensitivity (Figure 2a). Both of these regions (with the left region mirrored in the right hemisphere) contained the peak coordinates of Yeo et al.'s (2017) meta-analytically

identified right ITNA (MNI 55, -50, -12), suggesting that the regions could be considered ITNAs or at the very least contained the ITNAs. Nonetheless, as with the findings by Amalric and Dehaene (2016), the hemispheric asymmetry of the bilateral ITNAs found by Pollack and Price (2019) was also based on separate group-level analyses – one localized by a contrast of two conditions, and another by a brain-behavior correlation. Whether the functional and representational properties of the bilateral ITNAs differ *within an individual* remains unexplored.

Using the Triple-code Model as a framework, we speculated that the following non-mutually exclusive explanations might account for such a hemispheric asymmetry during visual search for digits observed by Pollack and Price (2019). The first possible explanation is that the left-hemispheric pathway may be recruited in most participants due to a reliance on the verbal system, possibly in retrieving the character names or identities as one scans the character string. Indeed, evidence from split-brain patients suggest a slight left-hemispheric advantage for the identification of digits (Cohen & Dehaene, 1996; Corballis, 1994; Seymour et al., 1994). The second possible explanation is that the right-hemispheric pathway may be less obligatory for a categorization task that does not require distinguishing between digits precisely (i.e., a digit was detected regardless of whether it was a 2 or a 7) but is almost always recruited in tasks in which the quantitative meanings or visuospatial aspects of numerals are necessary. In particular, reading numerals in many contexts involves precise place-value encoding. For example, ‘35’ is numerically different from ‘53’ even though they comprise the same digits. Whereas the left hemisphere may favor analytic processing of the decomposed digits, the right hemisphere may favor holistic processing of digit strings that integrates place values (Knops, Nuerk, Sparing, et al., 2006; Ratinckx et al., 2006). This may result in the predominance and a causal role of a right-hemispheric pathway in automatic magnitude processing of numerals (i.e., even when the quantitative meanings are irrelevant for an overlearned task). For example, Cohen Kadosh and

colleagues (2007, 2012) found that transcranial magnetic stimulation of the right intraparietal sulcus, but not the left, impaired automatic magnitude processing in a numerical Stroop task. Moreover, representations of numbers and space are inextricably related in the putative mental number line in which smaller numbers are represented to the left and larger numbers to the right (Hubbard et al., 2005), and visuospatial processing tends to be right lateralized (De Schotten et al., 2011; J. J. Vogel et al., 2003). Hence, it is reasonable to infer that semantic processing of numerals requires right hemisphere brain structures. Stimulation studies using transcranial magnetic or electrical stimulation have also revealed causal evidence of a right lateralization for number line bisection (perception of midpoint of number intervals) and place-value processing (Artemenko et al., 2015; for a recent review, see Faye et al., 2019; Göbel et al., 2006). Taken together, it is therefore plausible that individuals who are more skilled in calculation (most involve multi-digit numerals) would tend to automatically engage the right-hemispheric pathway to a greater extent.

It has also been proposed recently, as an extension to the Triple-code Model, that the left hemisphere may be recruited for numerical tasks that are more novel, attention-demanding and effortful (e.g., symbolic arithmetic), whereas the right hemisphere may be recruited for tasks that have been familiar, overlearned and automatized (recognizing digits) (for a review, see Arsalidou et al., 2018; Skagenholt et al., 2018). If the hypothesis were true, the digit detection task, which poses low difficulty for adults, should recruit the left ITG to a lower extent the right ITG. In contrast, performance on an out-of-scanner standardized assessment of calculation skills, which is a more difficult task than the in-scanner digit detection should be associated with greater activity in the left ITG rather than the right ITG. However, Pollack and Price's (2019) data do not seem to be consistent with both predictions from this hypothesis, at least not for the interior temporal nodes involved in the numerical tasks examined. Therefore, it is unlikely that the hemispheric asymmetry findings by

Pollack and Price (2019) could be fully accounted for by an effortful-automatic continuum of cognitive processing.

Current Study

In this study, we re-analyzed Pollack and Price's (2019) data with two aims. While Pollack and Price (2019) focused on *localization* of the ITNAs using mass-univariate voxel-wise analyses (i.e., the activation or response of each voxel is analyzed independently), our first aim was to use region-of-interest (ROI) based univariate analyses (i.e., taking the mean response across all voxels in a region specified a priori) and *within-participant* comparisons to further characterize the hemispheric asymmetries of the bilateral ITNAs in their digit sensitivities and their relation to symbolic calculation skills. Our second aim was to characterize any hemispheric asymmetries in the representational properties of the ITNAs indexed by multivoxel pattern analyses (i.e., the pattern of response across *multiple* voxels in a region is analyzed simultaneously) and to relate them to calculation skills. It is well demonstrated across several studies that univariate regional-average activation and multivariate pattern analyses can provide contrasting, but complementary information (Coutanche, 2013; Jimura & Poldrack, 2012; McGugin et al., 2015). This in-depth investigation of the functional and representational properties allows us to test and further inform models of numerical processing, such as the Triple-code Model.

Is There *Within-Individual* Hemispheric Asymmetry in the ITNAs' Digit Sensitivity?

Due to the original univariate findings (Pollack & Price, 2019), we predict that, on average, digit sensitivity will be greater in the left than in the right ITNA. We also predict that higher calculation skills will be associated with less left lateralization[2], or greater right lateralization.

[2] Conditioned on the observed positive correlation between calculation skills and digit sensitivity in the right IT reported by Pollack and Price (2019), an association between calculation skills and greater left lateralization would imply a stronger relation between calculation skills and digit sensitivity of the left ITNA than with the digit sensitivity of the right ITNA. This was, however, not the case.

Do the Multivoxel Patterns in the ITNAs Discriminate Between Digits and Letters?

Although the right ITNA did not appear to be sensitive to digits in terms of its regional mean response amplitude, an analysis of multivoxel response patterns may reveal category discriminability (Yeo et al., 2020). Specifically, the response patterns in the ITNAs evoked by each single target allow us to examine the multi-dimensional organization of exemplar-level neural representations – commonly referred to as "representational geometry" within the representational similarity analytic (RSA) framework (Kriegeskorte et al., 2008). With RSA, the neural representations of detected digit and letter targets could form separate clusters. Based on the original univariate finding on digit sensitivity, we predict that the left ITNA will show greater category discriminability than the right ITNA. However, based on prior meta-analytic and multivoxel pattern findings (Yeo et al., 2017, 2020), category discriminability could also be greater in the right than in the left ITNA. We also predict that higher calculation skills will be associated with greater category discriminability in both ITNAs, but we have no specific prediction for its laterality.

Do the Multivoxel Patterns in the ITNAs Discriminate Between Digit Exemplars?

Regardless of whether category discriminability was evident in the ITNAs, it would be informative to assess whether digit discriminability was evident. This is because the identity and category of a character are represented in parallel rather than serially (McCloskey & Schubert, 2014; Taylor, 1978). We predict that digit discriminability will be observed in both ITNAs, but it will be greater in the left than in the right ITNA. We also predict that higher calculation skills will be associated with greater digit discriminability in both ITNAs, but we have no specific prediction for its laterality.

Are Digit Representations Organized Similarly Between the ITNAs?

Finally, we explored whether we could describe the representational geometries using hypothetical or 'candidate' representational models. Given that the numeral identification systems function as an integrative network, the representational geometries being studied in the ITNAs likely reflect both bottom-up and top-down influences from the visual, verbal, and magnitude codes within each hemispheric pathway (Bar et al., 2006; Gwilliams & King, 2020; Kay & Yeatman, 2017; Price & Devlin, 2011). Given the left hemisphere's dominance for language processing and based on the Triple Code Model, we hypothesize that if response patterns in the left ITNA are primarily influenced by phonological representations from the verbal code, characters with similar phonological form will evoke similar response patterns in the left ITNA. On the other hand, if the response patterns in both ITNAs are primarily influenced by the magnitude code (Grotheer et al., 2018), we would expect digits that are numerically closer (e.g., 8 vs. 9) to evoke more similar response patterns than digits that are numerically distant (e.g., 2 vs. 9) (Piazza et al., 2007; S. E. Vogel et al., 2015, 2017). We also predict that higher calculation skills will be associated with greater dissimilarity in the representational geometries of digits in the ITNAs. In either case, we predict that the representational geometries in both ITNAs will not be adequately described by visual form similarity (Yeo et al., 2020).

Methods

We report how we determined our sample size, all data exclusions, all inclusion/exclusion criteria, whether inclusion/exclusion criteria were established prior to data analysis, all manipulations, and all measures in the study. No parts of the study procedures or analysis plans were preregistered prior to the research being conducted.

Participants

Thirty-two neurologically typical and right-handed adults (M_{Age} = 19.38, *SD* = 1.50, 21 females) were included in the current analyses. These are the exact same data that were analyzed in the initial univariate functional localization study by Pollack and Price (2019). The study was approved by the university's Institutional Review Board, and all participants gave written informed consent. As the current aims precluded a priori power analyses, we performed sensitivity analyses and reported them in the Supplemental Materials.

Tasks

fMRI Tasks

To localize digit-related vOT regions, participants completed visual search tasks involving alphanumeric characters in the MRI scanner. During digit detection, participants determined whether a digit was present among a string of letters (Figure 2a) by pressing one of two assigned buttons (i.e., one button for target present and another button for target absent). During letter detection, participants determined whether a letter was present among a string of digits (Figure 2b). The single target digit or letter, which could be digits 1 – 9 and letters A, C, D, E, H, R, N, S, and T, was presented in either the 2nd, 3rd, or 4th position of the 5-character string. Each target digit/letter exemplar was presented in three unique strings per run (see Table S1 for stimulus list). Each run comprised 16 s of fixation baseline at the start and the end of the run, and 54 trials (27 Target Present trials across all 9 digit/letter exemplars, and 27 Target Absent trials). On each trial, the character string was presented for 1 s, and the inter-stimulus interval was 2, 4, or 6 s (*M* = 4 s). Justifications for the design of the stimulus sets can be found in Pollack and Price (2019).

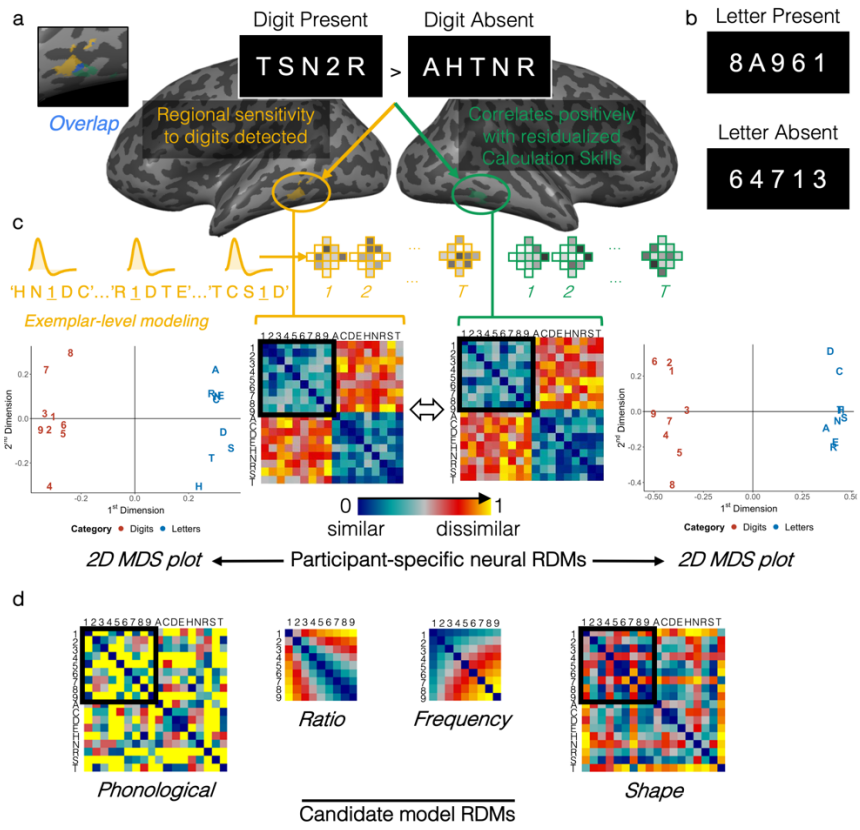

Figure 2. Regions of interest (ROIs) and a schematic of the representational similarity analyses (RSA). (a) Left and right IT ROIs from Pollack and Price (2019) derived from a random-effects analysis of [Digits Present > Digits Absent] contrast maps (yellow), a correlational analysis of those contrast maps with calculations skills (green), respectively, and their overlap (blue). (b) Example stimuli for letter detection task. (c) For each ROI, response patterns reliably evoked by correctly detected target across different character strings [Digit/Letter Present > Fixation] were correlated in a pairwise manner to construct participant-specific representational dissimilarity matrices (RDMs). Purely for representational purposes across different scales used for the neural and candidate model RDMs (see (d)), the RDM values were standardized to a range of 0 (similar) to 1 (dissimilar). 2D plots of the representational geometries in each ROI obtained by multidimensional scaling (MDS). The RDMs and MDS plots above are the group means for a representative illustration. Hemispheric asymmetry was assessed by correlating the (full or subset) RDMs of the left and right IT ROIs (e.g., black border indicates the Digits-only RDMs. (d) Candidate model RDMs. Black border indicates the Digits-only RDM.

All participants completed four runs each of digit detection and letter detection, hence, across all four runs, each target digit/letter exemplar was presented a total of 12 times. Based on pre-determined criteria for excessive motion (> 3 mm maximum displacement and/or three degrees of volume-to-volume displacement), one digit run and one letter run from one participant, and one letter

run from another participant, were excluded from the analyses in Pollack and Price (2019). Mean accuracies for the conditions critical to our key analyses (Digit Present and Letter Present) were at least 92%. See Table S3 for full descriptive statistics of the task performance, and Pollack and Price (2019) for analyses of the behavioral measures.

Standardized Cognitive Assessments

Calculations skills were measured using the Calculation and Math Fluency subtests of the Woodcock-Johnson III Tests of Achievement (WJ III ACH; Woodcock et al., 2001). The Calculation subtest is an untimed test that assesses arithmetic, algebra, trigonometry, and calculus. The Math Fluency subtest assesses the ability to solve as many simple addition, subtraction, and multiplication problems with the numerals 0–10 as possible within three minutes. A Calculation Skills cluster score was computed from a composite of Calculation and Math Fluency measures. As a proxy for domain-general symbol decoding, the Letter-Word Identification (ID) subtest of the WJ III ACH was used. The Letter-Word ID subtest is an untimed test that assesses the ability to read aloud a list of letters and words accurately. See Table S3 for descriptive statistics of these measures. For consistency with the original study, in all analyses involving the Calculation Skills cluster measure, we used the residuals after regressing the Calculation Skills standard scores on Letter-Word ID standard scores.

Legal copyright restrictions prevent public archiving of the subtests from the Woodcock-Johnson III Tests of Achievement, which can be obtained from the copyright holders in the cited references.

Neuroimaging Data Acquisition

Structural and functional brain images were acquired using a 3T Philips Intera Achieva scanner with a 32-channel head coil. High-resolution 3D anatomical scans were collected over approximately 6 min with TR/TE = 8.1/3.8 ms, flip angle = 5□, field of view (FOV) = 256 mm, and 1

mm isotropic voxels. T2*-weighted single-shot echo-planar imaging sequence functional images were acquired with TE = 25 ms, TR = 2000 ms, flip angle = 90□, FOV = 240 mm, matrix size = 96 × 96 mm, 2.5 × 2.5 × 3 mm^3 voxels, with 0.25 mm gap between the 3-mm thick slices, 40 slices, and 151 volumes per run. Five additional dummy volumes acquired at the start of each run to allow for steady-state magnetization were discarded.

fMRI Data Preprocessing

Structural and functional images were preprocessed and analyzed using BrainVoyager 20.4 (Brain Innovation, Inc., Maastricht, the Netherlands). Functional images were corrected for differences in slice time acquisition (cubic spline interpolation), head motion (trilinear-sinc interpolation), and high-pass filtered (GLM approach with Fourier basis set, 2 cycles) to remove linear and non-linear trends. Functional data were co-registered to the structural data using boundary-based registration, normalized to MNI space, and re-sampled to 3-mm isotropic voxels. Univariate analyses were conducted on spatially-smoothed data with a Gaussian kernel of 6 mm at full-width half-maximum. Multivariate analyses were conducted on spatially unsmoothed data.

Neuroimaging Statistical Modeling

Univariate Analyses

For each participant, all included runs were modeled with a two-gamma hemodynamic response function. The data were analyzed simultaneously using a random-effects multi-subject General Linear Model (GLM), corrected for serial correlations with a second-order autoregressive method. The GLM included a regressor each for Digit Present (correct only), Digit Absent (correct only), Letter Present (correct only), Letter Absent (correct only), errors of commission and omission, and six regressors of motion parameters (translational and rotational in *x*, *y*, and *z* axes) for each run.

Multivariate Analyses

Each of the nine target digit/letter exemplars was presented 12 times across all digit or letter detection runs. Given the presence of characters from the non-target category (e.g., letters in 'T S N 2 R' for digit detection) on each Target Present trial, we attempted to minimize the influence of the non-target characters in our analyses by modeling all instances of a target exemplar that was detected correctly across all runs (e.g., ['H N 1 D C', 'R 1 D T E', 'T C S 1 D'] × 3 or 4 runs to estimate the voxel-wise response to a detected '1'). This approach ensured that the voxel-wise responses estimated from the [Target Present - Fixation] contrast would be reliably specific to the target exemplar common to the modeled trials (see Figure 2c). However, as the original study was not designed with exemplar-level representations in mind, some characters from the non-target category always co-occurred with some of the target exemplars, such as 'D' was always present in all Digit Present trials with the target '1'. We reasoned that if the co-occurring characters were also reliably represented in the activation patterns of the target exemplar, then the activation pattern of the non-target character (e.g., 'D') would be highly similar to the activation pattern of the target exemplar (e.g., '1'). However, across all the affected pairs, we did not find any evidence that the target exemplar was no more correlated with the co-occurring non-target exemplar (e.g., '1' with 'D') than other non-co-occurring characters (e.g., '1' with 'H', 'N', 'C', etc.) (see supplemental analyses and Table S4). This suggests that the co-occurring characters were not reliably represented in the activation patterns of the target exemplar. These findings ruled out the possibility that the co-occurring characters from the non-target category might strongly influenced the results of the multivariate analyses.

To further ensure that we could reliably estimate the response patterns at the exemplar level for each participant, we used an arbitrary cut-off of 50% accuracy (i.e., at least 6 correct Target Present trials) per exemplar as an inclusion criterion for multivariate analyses. All participants but

one had at least six correct trials per digit/letter exemplar to reliably estimate an exemplar-level response pattern. That one participant had only 1 to 5 correct trials for 7 out of 9 letters. Hence, for all analyses involving letter exemplar representations, we excluded that participant. The mean number of remaining correct Target Present trials per exemplar was 11 for both digits and letters.

For each participant, all included runs were modeled with a two-gamma hemodynamic response function and analyzed simultaneously using a fixed-effects single-subject GLM, corrected for serial correlations with a second-order autoregressive method. The GLM included a regressor each for the nine target digits (correct only), a regressor for Digit Absent (correct only), a regressor for each of the nine target letters (correct only), a regressor for Letter Absent (correct only), four regressors for errors of commission and for omission (separately modeled for digit and letter detection), and six regressors of motion parameters for each run.

Regions of Interest (ROIs)

The current study is not only interested in how the left and right IT regions are functionally and representationally different, but also in *why they were localized in Pollack and Price (2019) in different ways*. Figure 2a shows the left and right IT functional (i.e., data-driven) ROIs from Pollack and Price (2019), which are used as proxies for the left and right ITNAs, respectively. Specifically, a *t*-test of [Digit Present > Digit Absent] contrast maps revealed a left IT cluster (but not in the right IT), and a brain-behavior correlation of the same contrast maps and residualized calculations skills scores revealed a right IT cluster (but not in the left IT). The statistical thresholds used for both analyses were identical: voxel-level threshold of $p < .005$, and cluster-level threshold of $p < .05$ via Monte Carlo simulations. The peaks of the ROIs are within □ 3 mm (i.e., one functional voxel) along each dimension (left: MNI -57, -52, -11 and right: MNI 54, -52, -14). Although both ROIs have 59 functional voxels, the spatial extents of the ROIs (left: 728 mm^3; right: 670 mm^3) are non-homotopic.

Flipping one ROI onto the other hemisphere revealed that the spatial overlap is about 15% (105 mm^3), which contains the meta-analytic peak of the ITNA from Yeo et al. (2017) (MNI 55, -50, -12) (see Figure 2a).

Statistical Analyses

Most of the analyses reported below pertain to the digit detection task. Where applicable, we also performed an identical set of analyses for the letter detection task to assess the category specificity of the digit-related findings. Detailed results of the letter detection task are reported in the Supplementary Materials.

Univariate Analyses

To fully characterize the IT ROIs in terms of their regional mean digit sensitivity (i.e., response amplitudes evoked by detected digits) beyond the findings reported by Pollack and Price (2019), we conducted the following post hoc analyses[3]: (1) We tested whether, on average, there was within-individual asymmetry in the left and right ITs' digit sensitivity (i.e., mean beta values from the [Digit Present – Digit Absent] contrast) (paired samples *t*-test, two-tailed); (2) We also probed whether the degree of right lateralization in the digit sensitivity was positively correlated with calculation skills. To compare the degree of lateralization across individuals normalized for individual differences in digit sensitivity, we computed a dissimilarity-like[4] laterality index, LI = $\frac{L-R}{\max(|L|,|R|)}$, where L and R are the mean digit sensitivity of the left and right ROIs, respectively (Seghier, 2019). A positive LI indicates left lateralization and a negative LI indicates right

[3] Although these analyses are post hoc and therefore non-independent from the analyses reported by Pollack and Price (2019), the authors did not compute a within-participant difference score to directly assess hemispheric asymmetry.

[4] A more widely used formula is LI = $\frac{L-R}{|L|+|R|}$ (for reviews, see Bradshaw et al., 2017; Seghier, 2008). This LI formula is typically used for classification purposes (left- or right-lateralized, or bilateral), but is problematic for analyses of individual differences because it lacks meaningful variation (Bradshaw et al., 2017; Jansen et al., 2006) and it is not a proper distance metric (Seghier, 2019).

lateralization. The participant-specific LI scores were then correlated with the residualized Calculation Skills scores (Pearson's correlation, one-tailed).

As the effects for the [Digit Present – Digit Absent] contrast could be driven by the Digit Present and/or Digit Absent condition, we further explored whether these predicted effects also pertained to the condition versus baseline contrasts (i.e., [Digit Present – Fixation] and [Digit Absent – Fixation]).

Representational Similarity Analyses

Neural Representational Dissimilarity Matrices (RDMs). For each participant and each ROI, the response pattern evoked by each correctly detected digit or letter exemplar from the [Digit/Letter Present – Fixation] contrast was characterized by the spatial distribution of *t*-values (Misaki et al., 2010) (Figure 2c). For each participant, some voxels might not have valid or complete functional data across all runs. To ensure comparable degrees of freedom across all voxels included in the statistical analyses, BrainVoyager applies an intensity threshold (an arbitrary units of 100) to exclude such voxels. All individual functional coverage maps were visually checked to determine that the threshold was reasonable for all subjects. Following the statistical computations, the values of these voxels in the statistical maps were set to zero across all conditions. As they do not contribute any information about condition-specific activation, they were considered non-informative. Non-informative voxels were excluded from subsequent analyses. This resulted in 53–59 voxels (M = 58.09) per participant for the left IT ROI, and 58–59 voxels (M = 58.97) per participant for the right IT ROI. We then computed the pairwise correlational distances (1 – Pearson's r) to construct participant-specific 18 × 18 representational dissimilarity matrices (Full-RDMs) for the left and right IT ROIs (Figure 2c). For all key analyses, we focused on the 9 × 9 Digits-RDMs (i.e., digits subset of the Full-RDMs; N = 32).

Category Discriminability. To assess the degree of category discriminability (digits versus letters) within each ROI, we computed a participant-specific category discriminability index (CDI) using the formula CDI = $M_{\text{between-category dissimilarities}} - M_{\text{within-category dissimilarities}}$ from the Full-RDM (Nili et al., 2020) after Fisher's *z* transformation of the *r* values. A higher CDI indicates greater category discriminability. We tested whether the mean CDI was statistically greater than zero (one-sample *t*-test, right-tailed). To also assess whether greater category discriminability in each ROI was associated with higher calculation skills, we correlated the participant-specific CDIs with the residualized Calculation Skills scores (Pearson's correlation, right-tailed). We also tested whether laterality of category discriminability (LI = $\frac{L-R}{\max(|L|,|R|)}$) was associated with higher calculation skills (Pearson's correlation, two-tailed).

Although both ROIs were either directly or indirectly localized using the contrast [Digit Present > Digit Absent] (and not [Letter Present > Letter Absent]), one might argue that univariate activation differences between digits and letters detected already presupposed category discriminability in these ROIs. However, these new analyses focused on the similarity of exemplar-level multivoxel response patterns for Target Present relative to baseline (e.g., how similar the response pattern for a detected '4' was to a detected 'N'). Moreover, their similarities were assessed using correlational distance, which standardizes the response amplitudes and therefore reduces the influence of mean amplitude differences.

Exemplar Discriminability. To assess the degree of exemplar discriminability[5] within each ROI, we first split each participant's data into two halves (i.e., odd runs and even runs), and computed the reliabilities of the response patterns between the two halves. We then performed

[5] "Exemplar discriminability" is used as a general term to refer to discriminability among digits, among letters, or among both digits and letters. Throughout the manuscript, we use "digit discriminability" and "letter discriminability" when we refer to discriminability among digits only and among letters only, respectively.

Fisher's z transformation of the r values and computed the correlational distance to construct a split-data RDM comprising within-exemplar dissimilarity estimates along the diagonal and between-exemplar dissimilarity estimates in the off-diagonals. Finally, we computed a participant-specific exemplar discriminability index (EDI) using the formula EDI = $M_{\text{between-exemplar dissimilarities}} - M_{\text{within-exemplar dissimilarities}}$ (Nili et al., 2020). A higher EDI indicates greater exemplar discriminability. We analyzed the EDI in an approach identical to that for CDI.

Two participants who did not have an equal number of even and odd runs for the digit and/or letter detection were excluded from the EDI analyses (final $N = 31$ for split-data Digits-RDMs, and $N = 30$ for split-data Letters-RDMs).

Hemispheric Asymmetry of Representational Geometries. For each individual, we computed the similarity between the Digits-RDMs of the left and right IT ROIs (one-half of each symmetric matrix) using Spearman's correlation followed by Fisher's z transformation (ρ_z). To assess our prediction that, on average, there was hemispheric asymmetry in the representational geometries, we compared the alternative hypothesis that the mean similarity > 0 to the null hypothesis that the mean similarity ≤ 0 (one-sample t-test, right-tailed). Next, to assess whether greater hemispheric asymmetry (i.e., lower similarity) in the representational geometries of digits was associated with higher calculation skills, we correlated the participant-specific similarity scores with the residualized Calculation Skills scores (Pearson's correlation, left-tailed).

Representational Content. To probe the representational content of each IT ROI, we constructed four candidate model RDMs that are characterized by similarity in phonology, numerical magnitude, frequency, and visual form (Figure 2d).

Phonological Model. We constructed an 18 × 18 phonological model RDM from an empirically derived character-name confusion matrix that described the perceptual confusion of

participants who were asked to identify a digit or letter aurally presented in noise (Hull, 1973). We converted the asymmetric similarity-based confusion matrix that comprises the frequencies of confusions between every stimulus-response pair (e.g., responding '8' to stimulus '6', or responding 'A' to stimulus '8') into a dissimilarity matrix.

Numerical Models. We constructed two 9 × 9 numerical model RDMs based on ratio and frequency, identical to those used by Lyons and Beilock (2018). The Ratio model is based on the ratio between the quantities represented by a pair of digits n_i and n_j as a measure of similarity, where ratio = $\frac{\min(n_i,n_j)}{\max(n_i,n_j)}$, and larger values indicate greater similarity. The RDM was derived using the inverse of the ratios such that larger values indicate greater dissimilarity. The Frequency model is based on the frequency of co-occurrence of any given pair of digits as a measure of similarity. According to Benford's (1938) law, the probability of encountering a given digit in the leftmost position of multi-digit numerals, P(n), is $log_{10}(n+1) - log_{10}(n)$ (also see Dehaene & Mehler, 1992). We then computed the probability of the joint frequency of each pair of digits using P(n_i) × P(n_j), where larger values indicate greater similarity (Lyons & Beilock, 2018). Likewise, the RDM was derived using the inverse of the probability of the joint frequency such that larger values indicate greater dissimilarity.

Visual Form Model. We constructed an 18 × 18 Shape model RDM using a computational algorithm that is based on the similarity in the "context" of sampled points on a shape (i.e., how one point relates to all other points on a shape) and the degree to which one shape has to be deformed to map onto another shape (Belongie et al., 2002). An identical model was used in an RSA study by Yeo and colleagues (2020; see Supplemental Materials for computational details).

Similarity Between Model RDMs. Figures S1 – S4 are multidimensional scaling plots that illustrate the 2D representational geometry of the digit and letter exemplars in each model. The

bivariate rank correlations of the models are reported in Table S2. No pairs of models are highly similar (ρs < .16), although the Ratio and Frequency models have a strong negative correlation (ρ = -.65). Hence, greater support for the Ratio model would likely indicate less support for the Frequency model, and vice versa.

Similarity Between Neural and Model RDMs. The degree to which the 9 × 9 neural Digits-RDMs can be described by each model RDM was examined using the RSA toolbox (Nili et al., 2014). We correlated the neural and model RDMs (only one-half of each symmetric matrix) using Spearman's rank correlation followed by Fisher's *z*-transformation. For each model, we tested whether the mean correlation coefficient was statistically greater than zero (one-sample *t*-test, right-tailed). To estimate the upper and lower bounds of the maximum similarity that any model could achieve given the degree of between-participant variability, a "noise ceiling" was computed using the approach proposed by Nili and colleagues (2014). We also tested (a) within each ROI, whether the mean correlation coefficients between any pair of models were statistically different, and (b) for each model, whether the mean correlation coefficients between the left and right ROIs were statistically different (paired-sample *t*-tests, two-tailed).

As the Phonological and Shape model RDMs are not category-specific, we also examined whether the 18 × 18 neural Full-RDMs (i.e., the whole alphanumeric set; see Figure 2c) were similar to the full versions of the Phonological and Shape model RDMs (Figure 2d).

We corrected for multiple comparisons separately for each group of tests by controlling for false-discovery rate (FDR) at $q < 0.05$ (Benjamini & Hochberg, 1995). All *p*-values reported in the Results section are uncorrected for multiple comparisons, and statistically significant ones were noted if they also survived an FDR-correction.

Handling of Bivariate Outliers

To assess the robustness of the correlation analyses to bivariate outliers, we used the Minimum Covariance Determinant approach to estimate the bivariate location and scatter from 75% of the data (i.e., assuming no more than 25% of outlying values), and a chi-square distribution (df = 2) with $\alpha = .001$ (99.9% percentile) as an outlier criterion (Leys et al., 2018, 2019). As there is no theoretical basis for deciding whether an outlier could rightfully belong to the distribution of interest, we reported the affected correlation coefficients with and without the outliers (i.e., "skipped correlation"; Rousselet & Pernet, 2012; Wilcox, 2004).

Comparison of Correlation Coefficients

As the difference between a pair of statistically significant and non-significant correlation coefficients may not be itself statistically significant (Gelman & Stern, 2006; Nieuwenhuis et al., 2011; Rousselet & Pernet, 2012), whenever necessary, we used the full suite of tests (e.g., Fisher's Z) in *R* package 'cocor' (Diedenhofen & Musch, 2015) to compare whether a pair of correlation coefficients differed significantly.

Bayesian Statistical Inferences

For all *t*-tests and correlations, we supplement the frequentist *p*-values with Bayes Factors to provide a more nuanced inference regarding the strength of the conclusion that can be inferred from the current data. More importantly, unlike *p*-values that is conditional on the assumption that the null is true (i.e., we can only reject, but not accept the null hypothesis), Bayes Factors do not depend on such an assumption and thus allow us to provide support for null findings.

Priors used for Bayesian *t*-tests and correlational analyses include a Cauchy distribution with a scale of 0.707 and a stretched beta prior width of 1, respectively. To facilitate Bayesian inferences for each test, we report the Bayes factor in favor of the hypothesis supported using the notation conventions in JASP (JASP Team, 2020): BF_{10} and BF_{01} for two-tailed tests, and BF_{+0}, BF_{-0}, BF_{0+}

and BF_{0-} for one-tailed tests. Whenever the evidence in support of one hypothesis relative to another is less than 3 times, we inferred that the evidence is inconclusive, and that the data are insensitive to the hypotheses tested (Dienes, 2016; Dienes & Mclatchie, 2018).

Results

Regional Mean Digit Sensitivity

In Pollack and Price (2019), the left IT ROI was localized by its high digit sensitivity (i.e., [Digit Present – Digit Absent] contrast), whereas the right IT ROI was localized separately by the relation between individual differences in digit sensitivity and calculation skills. Here, we probed whether these hemispheric differences would hold when we directly compare them *within* participants. On average, there was no hemispheric asymmetry in regional mean digit sensitivity (left: $M \square SD = 0.17 \square 0.22$; right: $M = 0.13 \square 0.46$, difference: $M = 0.05 \square 0.42$), $t(31) = 0.62$, $d_z = 0.11$, $p = .541$, $BF_{01} = 4.44$ (Figure 3a). However, individuals with higher calculation skills had greater right lateralization in their mean digit sensitivity, $r(30) = -.45$, $p = .009$, $BF_{10} = 5.69$ (Figure 3b).

Although individual differences in the [Digit Present – Digit Absent] contrast in the left IT did not correlate significantly with calculation skills in the original whole-brain correlational analysis reported by Pollack and Price (2019), we tested whether such a relation could be observed using an ROI approach. Digit sensitivity in the left IT was also positively correlated with calculation skills, $r(30) = .42$, $p = .008$, $BF_{+0} = 6.77$. However, the correlation coefficient for the left IT did not differ significantly from that for the right IT ($r(30) = .62$), ps $> .206$.

In sum, there was, on average, no hemispheric asymmetry in digit sensitivity, and no evidence that digit sensitivity in the left and right IT differed qualitatively in their relation to calculation skills. However, consistent with our prediction, the *within-individual difference* in the digit sensitivity between hemispheres was related to calculation skills.

As the [Digit Present – Digit Absent] contrast could be driven by Digit Present and/or Digit Absent, we probed the nature of involvement of the IT ROIs for each condition. Contrary to the findings above, the condition-wise regional mean response amplitudes were strongly right-lateralized for both Digit Present (left: $M = 0.21 \square 0.45$; right: $M = 0.88 \square 0.78$, difference: $M = -0.67 \square 0.72$) [$t(31) = -5.26$, $d_z = -0.93$, $p < .001$, $BF_{10} = 2061$] and Digit Absent (left: $M = 0.04 \square 0.44$; right: $M = 0.75 \square 0.64$, difference: $M = -0.72 \square 0.74$) [$t(31) = -5.48$, $d_z = -0.97$, $p < .001$, $BF_{10} = 3642$] (Figure 3c). Individuals with higher calculation skills had greater response amplitudes for Digit Present in the right IT, $r(30) = .48$, $p = .003$, $BF_{+0} = 16.93$. A similar relation was inconclusive in the left IT, $r(30) = .25$, $p = .084$, $BF_{0+} = 1.01$. However, these correlation coefficients did not differ significantly (ps > .182), suggesting no evidence of a qualitative difference. There was evidence that calculation skills were not positively correlated with the response amplitude for Digit Absent in the left IT [$r(30) = .05$, $p = .393$, $BF_{0+} = 3.64$], but whether a positive correlation between calculation skills and response amplitude for Digit Absent in the right IT was inconclusive [$r(30) = .14$, $p = .224$, $BF_{0+} = 2.24$; $r_{skipped}(28) = .37$, $p = .023$, $BF_{+0} = 2.98$]. These correlation coefficients did not differ significantly between the left and right IT (ps > .704; after exclusion of outliers: ps > .179). In sum, there was only conclusive evidence of an association between calculation skills and Digit Present responses in the right IT, and a lack of association between calculation skills and Digit Absent (i.e., letters only) responses in the left IT. The correlation coefficients also differed significantly between Digit Present and Digit Absent in both regions (left IT: ps < .026; right IT: ps < .002; after bivariate outlier exclusion, ps < .020). In sum, these findings suggest that the relations between calculation skills and response amplitudes were specific to the detection of digits and not driven by the Digit Absent condition.

Finally, there was weak to moderate evidence that individuals with higher calculation skills also had greater right lateralization in their mean response amplitudes for Digit Present [$r(30) = -.36$, $p = .042$, $BF_{10} = 1.58$; $r_{skipped}(29) = -.48$, $p = .006$, $BF_{10} = 8.03$]. There was evidence of a lack of a similar relation for Digit Absent [$r(30) = -.09$, $p = .621$, $BF_{01} = 4.05$] (Figure 3d). These correlation coefficients were significantly different regardless of outlier exclusion (ps < .011).

The above analyses were also conducted on letter sensitivity using the letter detection runs (see Supplementary Materials) to assess category-specificity. We found that the right-lateralization of condition-wise response amplitudes appeared to be related to the detection task in general, regardless of whether one was looking for digits or letters. By and large, we observed no conclusive or robust relations between response amplitudes during letter detection and calculation skills.

Taken together, although there was no hemispheric asymmetry in digit sensitivity, there was a strong right lateralization of IT activity during digit or letter detection more generally. Moreover, the relations between calculation skills and right lateralization in digit sensitivity were largely specific to the detection of digits.

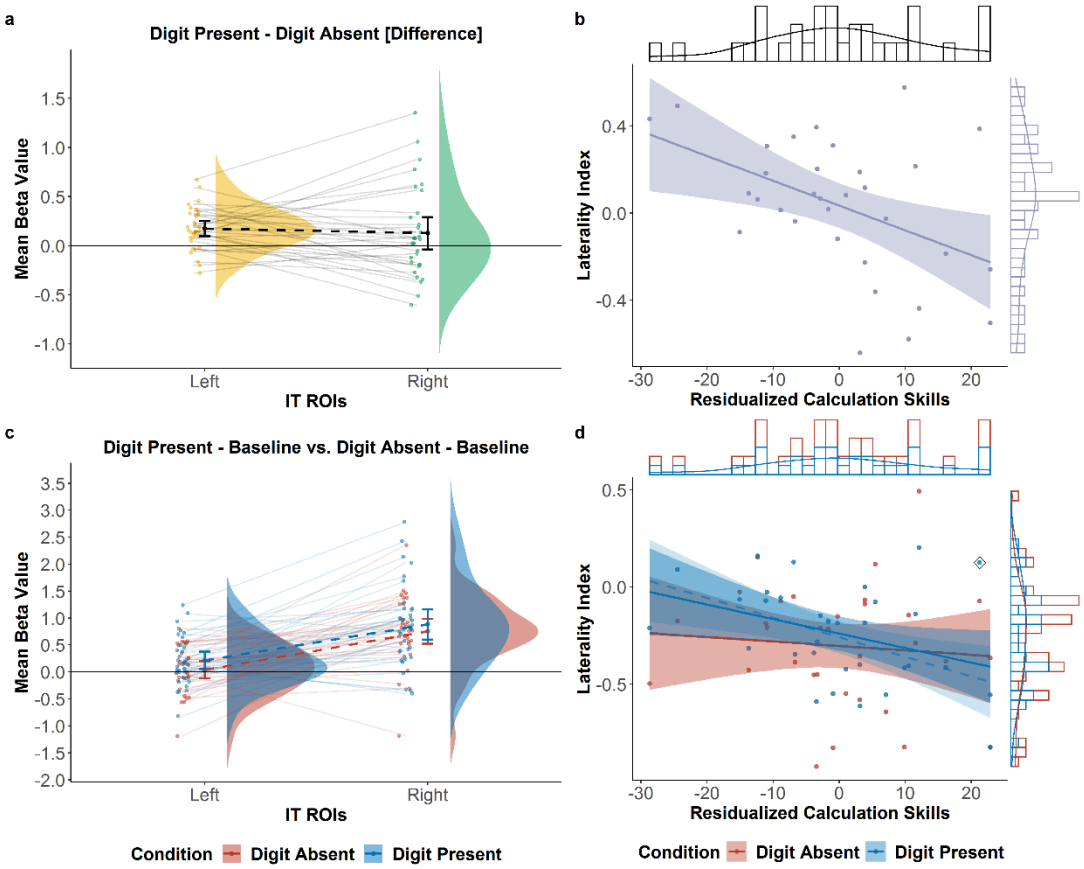

Figure 3. Hemispheric asymmetries of regional mean response amplitudes and their relation to calculation skills for digit detection. (a, b) digit sensitivity ([Digit Present – Digit Absent] contrast), and (c, d) condition-wise activity ([Digit Absent – Fixation] and [Digit Present – Fixation]). Error bars and bands are 95% confidence intervals. Dashed regression lines excluded bivariate outliers enclosed in ◇.

Category Discriminability (Digits vs. Letters)

Category discriminability between digits and letters was evident in both the left (M = 0.21 □ 0.08) [$t(30)$ = 15.07, d = 2.71, p < .001, BF_{+0} = 7.74×10^{12}] and right IT (M = 0.31 □ 0.11) [$t(30)$ = 15.55, d = 2.79, p < .001, BF_{+0} = 1.73×10^{13}] (Figure 4). Moreover, category discriminability was higher in the right IT than in the left IT (difference: M = -0.10 □ 0.11), $t(30)$ = -4.97, d_z = -0.89, p < .001, BF_{10} = 892.

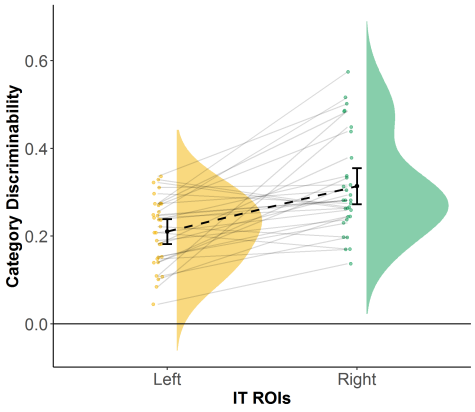

Figure 4. Category discriminability in the left and right IT ($N = 31$). Category discriminability was measured using $M_{\text{between-category dissimilarities}} - M_{\text{within-category dissimilarities}}$ from the Full-RDM. Error bars are 95% confidence intervals.

There was inconclusive evidence that greater category discriminability was associated with higher calculation skills in the left IT [$r(29) = .24$, $p = .102$, $BF_{+0} = 1.16$] and the right IT [$r(29) = .18$, $p = .170$, $BF_{0+} = 1.76$; $r_{skipped}(28) = .28$, $p = .069$, $BF_{+0} = 1.20$] (Figure 5). These correlation coefficients did not differ significantly (ps > .782). There was also no relation between the degree of lateralization of category discriminability and calculation skills, $r(29) = -.01$, $p = .938$, $BF_{01} = 4.47$].

In summary, not only was category discriminability robust in both ROIs, it was greater in the right IT than in the left IT. Whether greater category discriminability was associated with higher calculation skills was inconclusive. However, its lateralization did not matter.

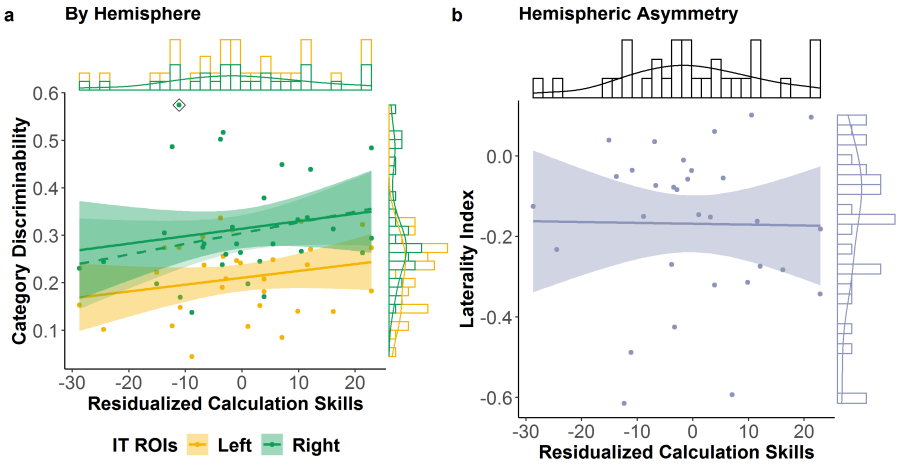

Figure 5. Relation between calculation skills and category discriminability (a) in left and right IT, and (b) its lateralization (negative: left lateralization, positive: right lateralization) ($N = 31$). Error bands are 95% confidence intervals. Dashed regression lines excluded bivariate outliers enclosed in ◇.

Digit (Exemplar) Discriminability

There was inconclusive evidence of digit discriminability in the left IT ($M = 0.008$ □ 0.06) [$t(30) = 0.73$, $d = 0.13$, $p = .234$, $BF_{0+} = 2.69$], and moderate evidence of a lack of digit discriminability in right IT ($M = 0.001$ □ 0.06) [$t(30) = 0.12$, $d = 0.02$, $p = .453$, $BF_{0+} = 4.75$] (Figure 6). However, there was no hemispheric asymmetry in digit discriminability (difference: $M = 0.006$ □ 0.08), $t(30) = 0.41$, $d_z = 0.07$, $p = .682$, $BF_{01} = 4.82$.

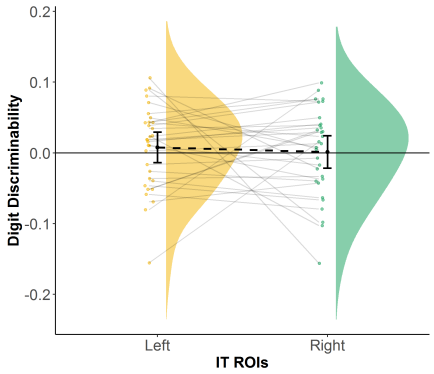

Figure 6. Digit discriminability in the left and right IT ($N = 31$). Digit discriminability was measured using $M_{\text{between-exemplar dissimilarities}} - M_{\text{within-exemplar dissimilarities}}$ across odd and even runs. Error bars are 95% confidence intervals.

Greater digit discriminability was, however, associated with higher calculation skills in the left IT [$r(29) = .38$, $p = .017$, $BF_{+0} = 3.83$], but evidence of a similar relation in the right IT was inconclusive [$r(29) = .17$, $p = .176$, $BF_{0+} = 1.81$] (Figure 7). These correlation coefficients did not differ significantly ($ps > .373$). There was also no relation between the degree of lateralization of digit discriminability and calculation skills [$r(29) = .13$, $p = .465$, $BF_{01} = 3.47$; $r_{skipped}(25) = .07$, $p = .744$, $BF_{01} = 3.98$]. Crucially, the significant correlation between digit discriminability in the left IT and calculation skills was not observed for letter discriminability (see Supplementary Materials; the correlation coefficients [Digit discriminability: $r(28) = .38$; Letter discriminability: $r(28) = -.21$] were significantly different, $ps < .012$).

In sum, although there was inconclusive evidence that the left IT distinguished digit exemplars on average across participants, there was evidence that the degree of distinction was associated with higher calculations skills. The right IT, on the other hand, did not distinguish digit exemplars, and had weaker, inconclusive evidence of a relation between digit discriminability and calculation skills.

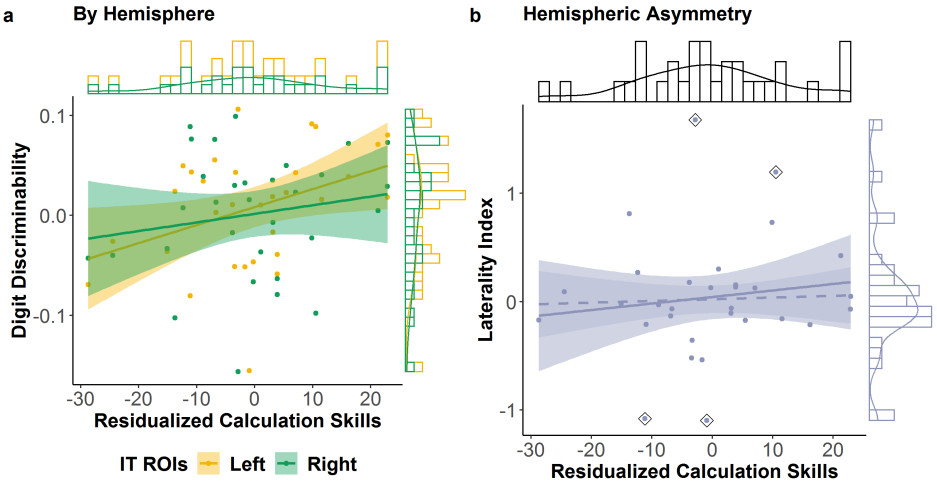

Figure 7. Relation between calculation skills and digit discriminability (a) in left and right IT, and (b) its lateralization (negative: left lateralization, positive: right lateralization) (N = 31). Error bands are 95% confidence intervals.

Hemispheric Asymmetry of Representational Geometries

On average, there was a small, but significant positive correlation between the representational geometries of digits (i.e., Digits-RDMs) in the left and right IT (mean ρ_z = .11 □ .20), $t(31) = 3.14$, $d = 0.56$, $p = .002$, $BF_{+0} = 20.51$. There was inconclusive evidence that lower between-hemisphere similarity (i.e., greater asymmetry) in the representational geometries of digits was associated with higher calculation skills, $r(30) = -.17$, $p = .172$, $BF_{0-} = 1.80$. A similar pattern of results was observed for the representational geometries of letters (see Supplemental Materials).

Representational Content

Digits

Although there was no evidence of digit discriminability in both IT ROIs, there could be a discernable organization among the exemplar representations regardless of how similar each exemplar pair was. Hence, we explored whether the representational geometries could be described by hypothesized models of phonological, numerical, and shape similarity.

Left IT. The left IT Digits-RDMs were not similar to the RDMs of the Phonological model (Mean ρ_z = -.01 □ .14) [$t(31) = -0.59$, $d = -0.10$, $p = .719$, $BF_{0+} = 7.84$], Ratio model (Mean ρ_z = -.01 □ .22) [$t(31) = -0.33$, $d = -0.06$, $p = .629$, $BF_{0+} = 6.70$], and Shape model (Mean ρ_z = -.05 □ .18) [$t(31) = -1.38$, $d = -0.24$, $p = .910$, $BF_{0+} = 11.55$] (Figure 8). There was, however, inconclusive evidence that the left IT Digits-RDMs were similar to the Frequency model RDM (Mean ρ_z = .09 □ .29), $t(31) = 1.69$, $d = 0.30$, $p = .051$, $BF_{+0} = 1.27$.

In terms of pairwise model comparisons, there was no evidence of within-participant differences between any pair of neural RDM-model RDM similarities, all *p*s > .052, BF_{10}s < 1.13 (Table S5).

Right IT. The right IT Digits-RDMs were not similar to the RDMs of the Phonological model (Mean ρ_z = -.03 □ .15) [$t(31)$ = -1.09, d = -0.19, p = .858, BF_{0+} = 10.19], Frequency model (Mean ρ_z = -.06 □ .20) [$t(31)$ = -1.63, d = -0.29, p = .943, BF_{0+} = 12.74], and Shape model (Mean ρ_z = -.04 □ .14) [$t(31)$ = -1.63, d = -0.29, p = .943, BF_{0+} = 12.76] (Figure 8). There was, however, inconclusive evidence that the right IT Digits-RDMs were similar to the Ratio model RDM (Mean ρ_z = .05 □ .19), $t(31)$ = 1.42, d = 0.25, p = .084, BF_{+0} = 1.18.

In terms of pairwise model comparisons, there was some evidence that the Digits-RDMs were more similar to the Ratio model RDM than to the Shape model RDM [$t(31)$ = 2.61, d = 0.46, p = .014, FDR-corrected p = .084, BF_{10} = 3.36], and no evidence of within-participant differences between any other pair of neural RDM-model RDM similarities [all *p*s > .076, BF_{10}s < 0.84] (Table S6).

In sum, there was evidence that the models could not adequately describe the representational geometries in both ROIs. However, there was an inconclusive trend for the fit of the Frequency model in the left IT and Ratio model in the right IT. Replicating Yeo and colleagues (2020), we found evidence of an absence of shape similarity in both regions.

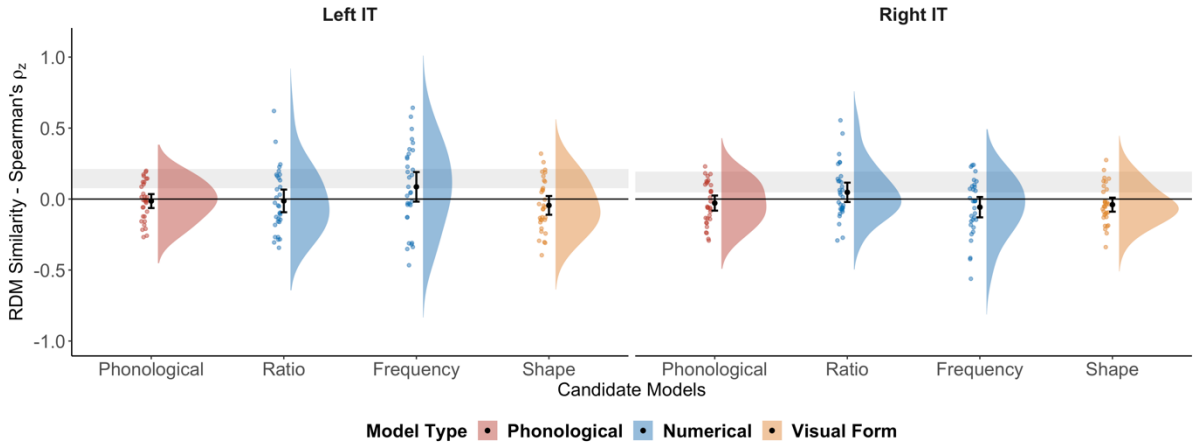

Figure 8. Similarity between the model RDMs and Digits-RDMs of the left and right IT ROIs (N = 32). Error bars are 95% confidence intervals. Grey bars indicate the estimated upper and lower bounds of the expected similarity achievable by the unknown true model given the degree of between-participant variability.

Left IT vs. Right IT. Neural RDM-model RDM similarities were not different between the left and right IT for the Phonological model [difference: M = 0.01 □ 0.16, $t(31)$ = 0.50, d_z = 0.09, p = .624, BF_{01} = 4.73] and Shape model [difference: M = -0.005 □ 0.22, $t(31)$ = -0.13, d_z = -0.02, p = .900, BF_{01} = 5.26] (Figure 9). There was inconclusive evidence that the neural RDM-model RDM similarities were different between the left and right IT for the Ratio model [difference: M = -0.06 □ 0.30, $t(31)$ = -1.15, d_z = -0.20, p = .259, BF_{01} = 2.90], and for the Frequency model [difference: M = 0.14 □ 0.36, $t(31)$ = 2.27, d_z = 0.40, p = .030 (FDR-corrected p = .120), BF_{10} = 1.75]. In sum, there was no hemispheric asymmetry in the degree to which the Phonological and Shape models described the representational geometries, but inconclusive evidence of hemispheric asymmetry for the Ratio and Frequency models.

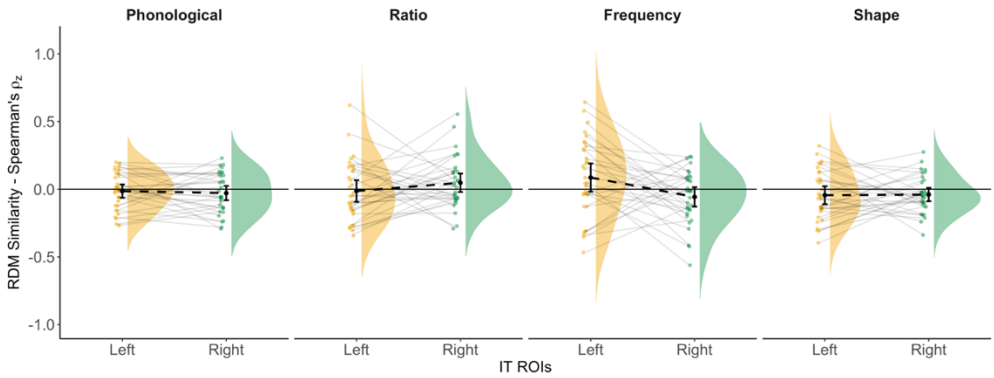

Figure 9. Hemispheric asymmetry in similarity between the model RDMs and neural Digits-RDMs (re-plotted from Figure 9) ($N = 32$). Error bars are 95% confidence intervals.

Alphanumeric Set

The Full-RDMs of the left and right IT were not similar to the Phonological and Shape model RDMs, $ps > .410$, $BFs_{0+} > 4.34$ (see Supplementary Materials). Taken together, phonological and shape information were not represented in either ROI regardless of whether digits were considered alone or simultaneously with letters.

Discussion

The present study applied both univariate and multivariate region-of-interest analyses to Pollack and Price's (2019) data to probe the hemispheric asymmetry of various functional and representational properties in the bilateral ITNAs during a digit detection task. We also probed the relation between those properties and calculation skills. Based on the findings of Pollack and Price (2019), we asked: Does the left ITNA show greater digit sensitivity than the right ITNA? Does the right ITNA relate to calculation skills in a way that the left ITNA does not? Here, we report that using univariate analyses (i.e., focusing on regional mean response amplitudes), the left and right ITNAs did not differ in their digit sensitivity and the relation between digit sensitivity and calculation skills. However, multivariate analyses (i.e., focusing on multivoxel response patterns) revealed that the right ITNA showed greater category discriminability between digits and letters. Greater right

lateralization of digit sensitivity and greater digit discriminability in the left ITNA were also related to higher calculation skills. Our findings thus suggest that the bilateral ITNAs are asymmetrically weighted in some functional responses and representations, at least during a digit detection task. However, until we have more convergent and conclusive evidence from future studies, the field should err on the side of caution and not readily generalize findings about one ITNA to the other.

Right ITNA is More Involved in Category Discrimination Than Left ITNA

First, contrary to our prediction, we found that the right IT region showed no less digit sensitivity than the left IT region when we directly compared their sensitivities within individuals. This suggests that the successful localization of digit sensitivity in the left IT (statistically significant), but not in the right IT (statistically non-significant) reported in Pollack and Price (2019) are not statistically different from each other.

However, using multivoxel pattern analyses, we found that both IT regions showed significant category discriminability between the alphabet and numerals, and the degree of category discriminability was greater in the right IT than in the left IT. Interestingly, further probing of the univariate analyses for each condition relative to the fixation baseline (e.g., Digit Absent > Fixation) revealed that the right IT region was substantially more engaged during visual search regardless of both the target category (i.e., digit or letter detection) and the presence or absence of a target. Taken together, these findings suggest that there may be an inherent task-related hemispheric asymmetry, and that the right ITNA is no less involved, if not more so, than the left ITNA in alphanumeric category discrimination. This right lateralization of alphanumeric category discrimination in the ITNAs is consistent with several studies (Yeo et al., 2017, 2020). Using similar representational similarity analyses, Yeo and colleagues (2020) found that a meta-analytic identified right ITNA discriminates digits from letters and novel characters that were passively viewed, but such evidence

was absent in its left mirrored homolog. However, it was unclear if a true hemispheric asymmetry exists because a direct comparison between the left and right ITNAs was not made in that study. Moreover, in a study by Grotheer, Ambrus and colleagues (2016), an application of transcranial magnetic stimulation to the right ITNA has been found to disrupt both letter and digit detection when participants were asked to categorize between alphanumeric characters and novel ones, suggesting a causal role of the right ITNA in alphanumeric categorization. Nonetheless, because Grotheer, Ambrus, and colleagues (2016) did not also stimulate the left ITNA, it is unclear whether the left ITNA plays a qualitatively similar, but weaker causal role in alphanumeric categorization.

Although the current study does not focus on functional localization, but on understanding the properties of the functionally localized regions by Pollack and Price (2019), our findings have implications on future localization studies. The results of the present study suggest that multivoxel pattern analyses do confer greater sensitivity than traditional univariate analyses, and they might be a powerful tool as a localization technique, especially for character categories that differ only by arbitrary representational purposes rather than inherent visual features. For instance, 5-7 year-old children who do not have a putative “Fusiform Face Area” based on univariate activation contrasts already show adult-like multivoxel pattern discrimination between faces and other categories in the most probable location of the “Fusiform Face Area” (Cohen et al., 2019). Hence, future studies that are unsuccessful in functionally localizing an ITNA using traditional univariate analyses may consider using a multivoxel pattern searchlight instead (e.g., see Carlos et al., 2019 for an example on localizing the "Visual Word Form Area").

Visual Search for Digits May Not Require Representations of Digit Identity in ITNAs

Even though there was evidence of category discriminability in both IT regions, we found no conclusive evidence of digit discriminability. This suggests that category representations can be

computed without minimal digit identity representations (i.e., one does not need to identify and verbalize which character it is in order to categorize it). Such a category distinction could simply be due to the spatial segregation of digit sensitivity (i.e., ITNAs) and letter sensitivity (i.e., "Visual Word Form Area" and "Letter Form Area") (Grotheer et al., 2018; Grotheer, Herrmann, et al., 2016; Pollack & Price, 2019). The dissociation between category identification and character identification is also consistent with existing behavioral evidence (McCloskey & Schubert, 2014; Taylor, 1978). McCloskey and Schubert (2014) showed that patient L.H.D., with alexia due to a left ventral lesion, was impaired in the ability to identify individual digits and letters but was perfectly accurate in classifying digits and letters in mixed strings (e.g., '2VG5QS'). The authors concluded that "digit/letter category representations and character identity representations were computed separately but concurrently for all elements in the display, with the category representations providing the basis for present/absent judgements when the target and distractors differed in category" (McCloskey & Schubert, 2014, p. 458). Psychophysics evidence in neurotypical adults also suggest that identity and category are extracted in parallel (Taylor, 1978).

It is important to note that our results demonstrate inconclusive evidence of digit discriminability in the left ITNA, but conclusive evidence of an absence of digit discriminability in the right ITNA and of hemispheric asymmetry in digit discriminability. It could be that visual search tasks that require basic level categorization (i.e., a digit or a letter) and not subordinate level categorization (i.e., which specific digit or letter) are not robust in eliciting digit identity representations. Nonetheless, it is possible that digit discriminability in the ITNAs would be robustly evident in tasks in which digit identity is crucial. For instance, Wilkey and colleagues (2020) found above-chance decoding of the multivoxel response patterns evoked by digits in the left mirrored homolog of the meta-analytically identified right ITNA (Yeo et al., 2017) across tasks involving

single-digit identification (Is it a 2?) and comparison to a reference magnitude (Is it greater or less than '5'?)[6]. Moreover, we found that digit discriminability in the left IT region was associated with calculation skills, which suggests that the discriminability of digit representations in the ITNAs do have behavioral relevance. The numerically weaker digit discriminability in the right IT in the current study and the study by Wilkey and colleagues (2020) is compatible with the hypothesis that the magnitude representations in the right intraparietal sulcus (to which the right ITNA is connected to; Abboud et al., 2015; Baek et al., 2018; Daitch et al., 2016; Nemmi et al., 2018), are more approximate, or less discrete, in nature compared to its left counterpart (Chassy & Grodd, 2012; Kimura, 1966; Kosslyn et al., 1989; Notebaert & Reynvoet, 2009; Piazza et al., 2006, 2007). Moreover, some studies that used transcranial magnetic stimulation (TMS) have also provided support for a critical causal role of the left hemisphere, particularly the left parietal cortex, in the discrimination of numerical symbols (Andres et al., 2005; for e review, see Faye et al., 2019; Göbel et al., 2001; Sandrini et al., 2004). For example, by applying TMS to either the left or right posterior parietal cortex, or both, Andres and colleagues (2005) found that although an approximate coding of digit magnitudes can be supported by either the left or right posterior cortex, the precise coding of digit magnitudes relies on the integrity of only the left posterior parietal cortex. Taken together, we speculate that the ITNAs may differ in how strongly they represent digit identity depending on the task context: When a task does not require discrimination between digits (e.g., category detection), digit identity is weakly represented in the ITNAs; when a task requires a digit to be discriminated from another digit (e.g., digit identification or magnitude comparison), digit identity is more strongly

[6] Above-chance decoding was found in the left ITNA (M = 27.8%, chance level = 25%), but not in the right ITNA (M = 26.6%). However, paired samples t-test revealed inconclusive evidence of whether the decoding accuracies were significantly different between hemispheres, $t(38) = 1.50$, $p = .143$, $BF_{01} = 2.05$.

represented in the ITNAs, possibly by top-down modulation. The extent to which the right ITNA discriminates digits may also be slightly weaker than that in the left ITNA.

Calculation Skills Are Associated with Hemispheric Asymmetry of Some Functional and Representational Properties

Using a region-of-interest analysis, we clarified that the mean digit sensitivity in the left IT region was also positively correlated with calculation skills, suggesting that the left IT region was not qualitatively different from the right IT region in its behavioral relevance, despite indications to that effect in the results reported by Pollack and Price (2019). Importantly, consistent with our prediction, we found that higher calculation skills were also associated with greater right lateralization in the digit sensitivity. Although our findings may not be consistent with Amalric and Dehaene's (2016) findings that the left (but not the right) ITNA's response to numerals was modulated by professional mathematical expertise, it is possible that a right lateralization in digit sensitivity is more robust within non-mathematicians, which can be observed in their data (Figure 8E).

We also found that greater digit discriminability in the left IT region was associated with higher calculation skills. This relation cannot be entirely explained by general symbol decoding because we regressed out letter-word identification skills from calculation skills. We also did not find a positive association between calculation skills and letter discriminability in both ROIs. Taken together, there is some degree of specificity between digit discriminability and calculation skills that is worth replicating in future research with a larger sample. Future work should also consider examining the relation between digit discriminability in the ITNAs and a behavioral measure of digit identification (e.g., under different levels of visual demands such as introducing noise or shortening presentation durations). It would also be necessary to control for general object recognition ability

(that is independent of intelligence) for which reliable individual differences have been found that generalize across familiar and novel object categories (Gauthier, 2018; Richler et al., 2017, 2019).

Although evidence for a similar relation between digit discriminability and calculation skills in the right IT region was inconclusive, we found that its correlational strength did not differ statistically from that in the left IT region, and that greater hemispheric asymmetry in digit discriminability was also not associated with higher calculation skills. Hence, it is possible that digit discriminability in the right IT region is as important for calculation skills as the left IT. Our findings are in contrast with a recent study by Wilkey and colleagues (2020) that found weak to moderate evidence of a null relation between decoding accuracy of multivoxel pattern classification of digit representations and calculation skills. One explanation is that the difference in tasks may modulate the degree of inter-individual variability in the discriminability of digit-specific representations. The digit detection task used here did not require discrimination between digits (i.e., whether the digit was a 2 or 3 did not matter), whereas Wilkey and colleagues (2020) used an identification task and a magnitude comparison task, for which discrimination between digits was necessary. It is possible that the digit detection task evoked spontaneous digit-specific representations with substantial inter-individual variability in the degree of discriminability. In contrast, in identification and comparison tasks, such inter-individual variability in the degree of discriminability may be attenuated when the digit-specific representations were amplified for further processing.

Finally, given the flexibility in the recruitment of either hemispheric number identification system depending on task contexts (Cohen & Dehaene, 1995, 1996, 2000), it is important to note that these findings may be specific to visual search tasks, and may not apply to other numerical tasks. Hence, more research would be needed to replicate and extend the current findings.

Inconclusive Evidence of Hemispheric Asymmetry in Representational Geometries of Digits in Both ITNAs

We explored whether there was a discernable organization in representational geometry of digits in each IT region that could be described by models that characterize phonological, numerical, or shape similarity, and whether the organization differed between hemispheres.

None of the models were adequate in describing the regions' representational geometries of digits. The null findings of the neural-and-model comparisons could possibly be explained by the lack of exemplar discriminability, which could result in noisy representational geometries without any meaningful rank order for the neural-and-model comparisons. As argued above, the lack of exemplar discriminability could be an artifact of the visual search paradigm rather than an intrinsic property of the ITNAs, or a lack of statistical power at the trial level given the split-half approach in computing the exemplar discriminability index. Given these caveats, we refrain from making any inferences about what the ITNAs represent. Nonetheless, there was conclusive evidence that the representational geometry of digits could not be described by visual form, which replicates the finding by Yeo and colleagues (2020). Hence, the prevalent label "Number Form Area" should be avoided since, to the best our knowledge, there is currently no direct evidence that numeral-preferring IT regions are sensitive to visual form per se (i.e., the actual physical shape of the digit) (Yeo et al., 2020), nor that systematic differences in visual form between letters and digits even exist (Schubert, 2017).

The current study also provides some indication of a ratio-based representational geometry that favored the right IT and a frequency-based representational geometry that favored the left IT. Although the evidence is inconclusive, the trends observed are consistent with current ideas of the emergence of brain networks underlying numerical cognition – a parietal "approximate magnitude

system" that is initially right-lateralized in infants and preschoolers, but becomes more bilateral with exposure to and development in symbolic numerical and mathematical knowledge (Edwards et al., 2016; Emerson & Cantlon, 2015; Hyde, 2021; Hyde et al., 2010). The decrease in laterality is thought to be partly due to the development of a left-hemispheric number system to support the representation of verbally anchored numerical symbols (Ansari, 2008; Holloway et al., 2010; Hyde, 2021). Importantly, numerals are encountered in our environments with highly predictable frequencies of co-occurrence (Dehaene & Mehler, 1992; Kojouharova & Krajcsi, 2019; Krajcsi et al., 2016) and thus it is not surprising that the representational geometry of digits may be shaped by the frequency of co-occurrences.

In sum, the insensitivity of the current data to disambiguate the various models suggests that more research needs to be conducted to examine hemispheric asymmetry or lack thereof in the representational geometries of digits in the ITNAs.

Limitations

First, it is possible the presence of other characters from the non-target category could have led to noisy exemplar-level representations. Although a single-character categorization task would be ideal to minimize the influence of characters from the non-target category, the present study was meant as a case study to probe a very specific hemispheric asymmetry reported by Pollack and Price (2019), so we were necessarily constrained by their experimental design. Future studies should consider designs with a single-stimulus presentation as well as a task that requires explicit digit discrimination to better understand the representational geometries of digits in the ITNAs.

Second, the present study focused only on the ITNA rather than also on the regions subserving the verbal and magnitude codes. Lateralization has been shown to be a regional-level phenomenon (i.e, lateralization may manifest in some regions, but not others; Pinel & Dehaene,

2010), so a focal analysis solely on the ITNAs is an appropriate first step for understanding the shared and distinct roles of the bilateral ITNAs. Besides, localization of regions underlying the verbal and magnitude codes is non-trivial without additional localizer tasks to isolate their respective representations. Given the hypothesized intra-hemispheric interaction between codes, future studies should also examine if hemispheric asymmetries in representational properties exist in the parietal regions subserving the magnitude code, and how they relate to the asymmetries between the ITNAs. Future studies should also consider a searchlight approach to localize neighboring sub-regions in the inferior temporal, parietal and frontal cortices that process different aspects of Arabic numerals. A collective effort of using different methodologies and analytical techniques will help advance the theories of numerical cognition.

Third, we used group-level ROIs because the right IT ROI was localized using a correlational approach at the group level. However, such group-level ROIs are less optimal and sensitive than subject-specific ROIs because they do not account for anatomical variability between individuals (Nieto-Castañón & Fedorenko, 2012). This may partly explain the difference in conclusions drawn here and from previous studies that utilize subject-specific ROIs and found that the bilateral ITNAs do not have distinct functional profiles (Grotheer et al., 2018; Grotheer, Herrmann, et al., 2016). Future research free of such methodological constraints should consider using subject-specific ROIs instead and probe the functional and representational properties across different tasks that vary in their verbal and magnitude processing demands.

Fourth, like many studies in cognitive neuroscience, the sample only included right-handed individuals. As handedness is closely tied to functional lateralization (e.g., Artemenko et al., 2020), the current evidence of patterns of hemispheric asymmetry in right-handers should not be

overgeneralized to the entire human population. Future studies should include left-handed and mixed handed individuals (Willems et al., 2014).

Conclusions

To explore how the bilateral ITNAs may be functionally dissimilar, we probed whether hemispheric asymmetry exist in an array of functional and representational properties of the ITNAs during a visual search task. In general, the ITNAs appear differentially weighted between hemispheres in some of their functional responses and representations that warrant caution in generalizing the findings of the ITNA in one hemisphere to the other. We found that the bilateral ITNAs did not differ in their sensitivity to digits, and that digit sensitivity in both ITNAs correlated positively with calculation skills. The differences between these findings and those originally reported by Pollack and Price (2019) suggest that within-individual comparisons are a necessary follow-up to infer hemispheric asymmetries. Nonetheless, we did uncover strong hemispheric asymmetry (right lateralization) in other properties, such as activity in alphanumeric categorization in general, as well as category discriminability. We also found certain properties that were associated with calculation skills, such as right-lateralization of digit sensitivity, and digit discriminability in the left ITNA. Given the hypothesis of flexible, task-dependent engagement of the bilateral ITNAs, our results are likely specific to visual search. Other numerical tasks may uncover hemispheric asymmetries in a similar or different set of properties of the bilateral ITNAs as we have found here. Hence, further investigation may be worthwhile to probe the individual and joint contributions of both hemispheres in processing numerals. Finally, to better understand the nature of hemispheric asymmetry of cognitive functions in general, our study highlights the need to supplement traditional univariate group-averaged analyses with within-participant comparisons, multivoxel pattern analyses, and individual differences analyses.

Funding

This work was supported by the National Science Foundation grants (DRL 1660816 and DRL 1750213) awarded to G.R.P, and the Humanities, Arts, and Social Sciences International PhD Scholarship (Nanyang Technological University and the Ministry of Education: Singapore) awarded to D.J.Y.

CRediT Authorship Contribution

Darren J. Yeo: Conceptualization, Methodology, Data curation, Software, Formal analysis, Writing - original draft, Writing - review & editing, Visualization, Funding acquisition. Courtney Pollack: Conceptualization, Methodology, Investigation, Data curation, Software, Formal analysis, Writing - review & editing. Benjamin N. Conrad: Conceptualization, Writing - review & editing. Gavin R. Price: Conceptualization, Methodology, Investigation, Writing - review & editing, Supervision, Project administration, Funding acquisition.

Data and Code Availability

The conditions of our ethics approval do not permit public archiving of anonymized raw MRI data because consent had only been obtained for study participation and not sharing of data with third parties. Readers seeking access to the raw MRI data should contact the corresponding author, Gavin R. Price. To obtain the data on request, a formal data sharing agreement must be signed, and participants must be contacted to provide consent for data sharing. However, we cannot guarantee that participants can still be contacted as data were collected in 2016 and 2017, and none of the authors are currently affiliated with the university in which ethics approval was obtained. Nonetheless, anonymized behavioral data, anonymized processed data from regions of interests that are less prone to identification, as well as processing and analysis scripts reported in the current study are publicly available at https://osf.io/7tjxz/ (DOI: 10.17605/OSF.IO/7TJXZ).

Acknowledgements

We would like to thank Andrew C. Lynn, Isabel Gauthier, James R. Booth, Laurie E. Cutting for their valuable feedback on previous versions of this work.

Conflict of Interest

We wish to confirm that there are no known conflicts of interest associated with this publication and there has been no significant financial support for this work that could have influenced its outcome.

References

Abboud, S., Maidenbaum, S., Dehaene, S., & Amedi, A. (2015). A number-form area in the blind. *Nature Communications*, *6*(1), 6026. https://doi.org/10.1038/ncomms7026

Amalric, M., & Dehaene, S. (2016). Origins of the brain networks for advanced mathematics in expert mathematicians. *Proceedings of the National Academy of Sciences*, *113*(18), 4909–4917. https://doi.org/10.1073/pnas.1603205113

Andres, M., Seron, X., & Olivier, E. (2005). Hemispheric lateralization of number comparison. *Cognitive Brain Research*, *25*(1), 283–290. https://doi.org/10.1016/j.cogbrainres.2005.06.002

Ansari, D. (2008). Effects of development and enculturation on number representation in the brain. *Nature Reviews Neuroscience*, *9*(4), 278–291. https://doi.org/10.1038/nrn2334

Arsalidou, M., Pawliw-Levac, M., Sadeghi, M., & Pascual-Leone, J. (2018). Brain areas associated with numbers and calculations in children: Meta-analyses of fMRI studies. *Developmental Cognitive Neuroscience*, *30*, 239–250. https://doi.org/10.1016/j.dcn.2017.08.002

Artemenko, C., Moeller, K., Huber, S., & Klein, E. (2015). Differential influences of unilateral tDCS over the intraparietal cortex on numerical cognition. *Frontiers in Human Neuroscience*, *9*, 1–8. https://doi.org/10.3389/fnhum.2015.00110

Artemenko, C., Sitnikova, M. A., Soltanlou, M., Dresler, T., & Nuerk, H. (2020). Functional lateralization of arithmetic processing in the intraparietal sulcus is associated with handedness. *Scientific Reports*, *10*(1), 1775. https://doi.org/10.1038/s41598-020-58477-7

Aurtenetxe, S., Molinaro, N., Davidson, D., & Carreiras, M. (2020). Early dissociation of numbers and letters in the human brain. *Cortex*, *130*(May), 192–202. https://doi.org/10.1016/j.cortex.2020.03.030

Baek, S., Daitch, A. L., Pinheiro-Chagas, P., & Parvizi, J. (2018). Neuronal Population Responses in the Human Ventral Temporal and Lateral Parietal Cortex during Arithmetic Processing with Digits and Number Words. *Journal of Cognitive Neuroscience*, *30*(9), 1315–1322. https://doi.org/10.1162/jocn_a_01296

Bar, M., Kassam, K. S., Ghuman, A. S., Boshyan, J., Schmidt, A. M., Dale, A. M., Hämäläinen, M. S., Marinkovic, K., Schacter, D. L., Rosen, B. R., & Halgren, E. (2006). Top-down facilitation of visual recognition. *Proceedings of the National Academy of Sciences of the United States of America*, *103*(2), 449–454. https://doi.org/10.1073/pnas.0507062103

Basso, G., Nichelli, P., Wharton, C. M., Peterson, M., & Grafman, J. (2003). Distributed neural systems for temporal production: A functional MRI study. *Brain Research Bulletin*, *59*(5), 405–411. https://doi.org/10.1016/S0361-9230(02)00941-3

Belongie, S., Malik, J., & Puzicha, J. (2002). Shape matching and object recognition using shape contexts. *IEEE Transactions on Pattern Analysis and Machine Intelligence*, *24*(4), 509–522. https://doi.org/10.1109/34.993558

Benford, F. (1938). The Law of Anomalous Numbers. *Proceedings of the American Philosophical Society*, *78*(4), 551–572.

Benjamini, Y., & Hochberg, Y. (1995). Controlling the false discovery rate: a practical and powerful approach to multiple testing. *Journal of the Royal Statistical Society*, *57*(1), 289–300.

Bradshaw, A. R., Bishop, D. V. M., & Woodhead, Z. V. J. (2017). Methodological considerations in assessment of language lateralisation with fMRI: a systematic review. *PeerJ*, *5*(7), e3557. https://doi.org/10.7717/peerj.3557

Bugden, S., Woldorff, M. G., & Brannon, E. M. (2019). Shared and distinct neural circuitry for nonsymbolic and symbolic double-digit addition. *Human Brain Mapping*, *40*(4), 1328–1343.

https://doi.org/10.1002/hbm.24452
Carlos, B. J., Hirshorn, E. A., Durisko, C., Fiez, J. A., & Coutanche, M. N. (2019). Word inversion sensitivity as a marker of visual word form area lateralization: An application of a novel multivariate measure of laterality. *NeuroImage*, *191*(August 2018), 493–502. https://doi.org/10.1016/j.neuroimage.2019.02.044
Carreiras, M., Monahan, P. J., Lizarazu, M., Duñabeitia, J. A., & Molinaro, N. (2015). Numbers are not like words: Different pathways for literacy and numeracy. *NeuroImage*, *118*, 79–89. https://doi.org/10.1016/j.neuroimage.2015.06.021
Carreiras, M., Quiñones, I., Hernández-Cabrera, J. A., & Duñabeitia, J. A. (2015). Orthographic Coding: Brain Activation for Letters, Symbols, and Digits. *Cerebral Cortex*, *25*(12), 4748–4760. https://doi.org/10.1093/cercor/bhu163
Chassy, P., & Grodd, W. (2012). Comparison of quantities: Core and format-dependent regions as revealed by fMRI. *Cerebral Cortex*, *22*(6), 1420–1430. https://doi.org/http://dx.doi.org/10.1093/cercor/bhr219
Cohen Kadosh, R., Bien, N., & Sack, A. T. (2012). Automatic and Intentional Number Processing Both Rely on Intact Right Parietal Cortex: A Combined fMRI and Neuronavigated TMS Study. *Frontiers in Human Neuroscience*, *6*, 1–9. https://doi.org/10.3389/fnhum.2012.00002
Cohen Kadosh, R., Cohen Kadosh, K., Schuhmann, T., Kaas, A., Goebel, R., Henik, A., & Sack, A. T. (2007). Virtual Dyscalculia Induced by Parietal-Lobe TMS Impairs Automatic Magnitude Processing. *Current Biology*, *17*(8), 689–693. https://doi.org/10.1016/j.cub.2007.02.056
Cohen, L., & Dehaene, S. (1991). Neglect Dyslexia for Numbers? A Case Report. *Cognitive Neuropsychology*, *8*(1), 39–58. https://doi.org/10.1080/02643299108253366
Cohen, L., & Dehaene, S. (1995). Number processing in pure alexia: The effect of hemispheric asymmetries and task demands. *Neurocase*, *1*(2), 121–137. https://doi.org/10.1080/13554799508402356
Cohen, L., & Dehaene, S. (1996). Cerebral networks for number processing: Evidence from a case of posterior callosal lesion. *Neurocase*, *2*(November), 155–174. https://doi.org/10.1080/13554799608402394
Cohen, L., & Dehaene, S. (2000). Calculating without reading: Unsuspected residual abilities in pure alexia. *Cognitive Neuropsychology*, *17*(6), 563–583. https://doi.org/10.1080/02643290050110656
Cohen, M. A., Dilks, D. D., Koldewyn, K., Weigelt, S., Feather, J., Kell, A. J., Keil, B., Fischl, B., Zöllei, L., Wald, L., Saxe, R., & Kanwisher, N. (2019). Representational similarity precedes category selectivity in the developing ventral visual pathway. *NeuroImage*, *197*, 565–574. https://doi.org/10.1016/j.neuroimage.2019.05.010
Colvin, M. K., Funnell, M. G., & Gazzaniga, M. S. (2005). Numerical processing in the two hemispheres: Studies of a split-brain patient. *Brain and Cognition*, *57*(1), 43–52. https://doi.org/http://dx.doi.org/10.1016/j.bandc.2004.08.019
Conrad, B. N., Wilkey, E. D., Yeo, D. J., & Price, G. R. (2020). Network topology of symbolic and nonsymbolic number comparison. *Network Neuroscience*, *4*(3), 714–745. https://doi.org/10.1162/netn_a_00144
Corballis, M. C. (1994). Can commissurotomized subjects compare digits between the visual fields? *Neuropsychologia*, *32*(12), 1475–1486. https://doi.org/10.1016/0028-3932(94)90119-8
Coutanche, M. N. (2013). Distinguishing multi-voxel patterns and mean activation: Why, how, and what does it tell us? *Cognitive, Affective and Behavioral Neuroscience*, *13*(3), 667–673. https://doi.org/10.3758/s13415-013-0186-2

Cui, J., Yu, X., Yang, H., Chen, C., Liang, P., & Zhou, X. (2013). Neural correlates of quantity processing of numeral classifiers. *Neuropsychology*, *27*(5), 583–594. https://doi.org/http://dx.doi.org/10.1037/a0033630

Cummine, J., Chouinard, B., Szepesvari, E., & Georgiou, G. K. K. G. K. (2015). An examination of the rapid automatized naming–reading relationship using functional magnetic resonance imaging. *Neuroscience*, *305*, 49–66. https://doi.org/10.1016/j.neuroscience.2015.07.071

Daitch, A. L., Foster, B. L., Schrouff, J., Rangarajan, V., Kaşikçi, I., Gattas, S., & Parvizi, J. (2016). Mapping human temporal and parietal neuronal population activity and functional coupling during mathematical cognition. *Proceedings of the National Academy of Sciences*, *113*(46), E7277–E7286. https://doi.org/10.1073/pnas.1608434113

De Schotten, M. T., Dell'Acqua, F., Forkel, S. J., Simmons, A., Vergani, F., Murphy, D. G. M., & Catani, M. (2011). A lateralized brain network for visuospatial attention. *Nature Neuroscience*, *14*(10), 1245–1246. https://doi.org/10.1038/nn.2905

Dehaene, S. (1992). Varieties of numerical abilities. *Cognition*, *44*(1–2), 1–42. https://doi.org/10.1016/0010-0277(92)90049-N

Dehaene, S. (1996). The Organization of Brain Activations in Number Comparison: Event-Related Potentials and the Additive-Factors Method. *Journal of Cognitive Neuroscience*, *8*(1), 47–68. https://doi.org/10.1162/jocn.1996.8.1.47

Dehaene, S., & Changeux, J. P. (1993). Development of elementary numerical abilities: a neuronal model. *Journal of Cognitive Neuroscience*, *5*(4), 390–407. https://doi.org/10.1162/jocn.1993.5.4.390

Dehaene, S., & Cohen, L. (1995). Towards an anatomical and functional model of number processing. *Mathematical Cognition*, *1*(1), 83–120.

Dehaene, S., & Cohen, L. (1997). Cerebral Pathways for Calculation: Double Dissociation between Rote Verbal and Quantitative Knowledge of Arithmetic. *Cortex*, *33*(2), 219–250. https://doi.org/10.1016/S0010-9452(08)70002-9

Dehaene, S., & Cohen, L. (2011). The unique role of the visual word form area in reading. *Trends in Cognitive Sciences*, *15*(6), 254–262. https://doi.org/10.1016/j.tics.2011.04.003

Dehaene, S., & Mehler, J. (1992). Cross-linguistic regularities in the frequency of number words. *Cognition*, *43*(1), 1–29. https://doi.org/10.1016/0010-0277(92)90030-L

Diedenhofen, B., & Musch, J. (2015). cocor: A Comprehensive Solution for the Statistical Comparison of Correlations. *PLoS ONE*, *10*(4), e0121945. https://doi.org/10.1371/journal.pone.0121945

Dienes, Z. (2016). How Bayes factors change scientific practice. *Journal of Mathematical Psychology*, *72*, 78–89. https://doi.org/10.1016/j.jmp.2015.10.003

Dienes, Z., & Mclatchie, N. (2018). Four reasons to prefer Bayesian analyses over significance testing. *Psychonomic Bulletin & Review*, *25*(1), 207–218. https://doi.org/10.3758/s13423-017-1266-z

Edwards, L. A., Wagner, J. B., Simon, C. E., & Hyde, D. C. (2016). Functional brain organization for number processing in pre-verbal infants. *Developmental Science*, *19*(5), 757–769. https://doi.org/10.1111/desc.12333

Emerson, R. W., & Cantlon, J. F. (2015). Continuity and change in children's longitudinal neural responses to numbers. *Developmental Science*, *18*(2), 314–326. https://doi.org/10.1111/desc.12215

Faye, A., Jacquin-Courtois, S., Reynaud, E., Lesourd, M., Besnard, J., & Osiurak, F. (2019). Numerical cognition: A meta-analysis of neuroimaging, transcranial magnetic stimulation and

brain-damaged patients studies. *NeuroImage: Clinical*, *24*(March), 102053. https://doi.org/10.1016/j.nicl.2019.102053

Fernandes, M. A., Moscovitch, M., Ziegler, M., & Grady, C. (2005). Brain regions associated with successful and unsuccessful retrieval of verbal episodic memory as revealed by divided attention. *Neuropsychologia*, *43*(8), 1115–1127. https://doi.org/http://dx.doi.org/10.1016/j.neuropsychologia.2004.11.026

Fias, W., Lammertyn, J., Caessens, B., & Orban, G. A. (2007). Processing of abstract ordinal knowledge in the horizontal segment of the intraparietal sulcus. *The Journal of Neuroscience*, *27*(33), 8952–8956. https://doi.org/http://dx.doi.org/10.1523/JNEUROSCI.2076-07.2007

Gauthier, I. (2000). What constrains the organization of the ventral temporal cortex? *Trends in Cognitive Sciences*, *4*(1), 1–2. https://doi.org/10.1016/S1364-6613(99)01416-3

Gauthier, I. (2018). Domain-Specific and Domain-General Individual Differences in Visual Object Recognition. *Current Directions in Psychological Science*, *27*(2), 97–102. https://doi.org/10.1177/0963721417737151

Gazzaniga, M. S., & Smylie, C. S. (1984). Dissociation of Language and Cognition. *Brain*, *107*(1), 145–153. https://doi.org/10.1093/brain/107.1.145

Gelman, A., & Stern, H. (2006). The difference between "significant" and "not significant" is not itself statistically significant. *American Statistician*, *60*(4), 328–331. https://doi.org/10.1198/000313006X152649

Glezer, L. S., & Riesenhuber, M. (2013). Individual Variability in Location Impacts Orthographic Selectivity in the "Visual Word Form Area." *Journal of Neuroscience*, *33*(27), 11221–11226. https://doi.org/10.1523/JNEUROSCI.5002-12.2013

Göbel, S. M., Calabria, M., Farnè, A., & Rossetti, Y. (2006). Parietal rTMS distorts the mental number line: Simulating "spatial" neglect in healthy subjects. *Neuropsychologia*, *44*(6), 860–868. https://doi.org/10.1016/j.neuropsychologia.2005.09.007

Göbel, S. M., Walsh, V., & Rushworth, M. F. S. (2001). The mental number line and the human angular gyrus. *NeuroImage*, *14*(6), 1278–1289. https://doi.org/10.1006/nimg.2001.0927

Goffin, C., Sokolowski, H. M., Slipenkyj, M., & Ansari, D. (2019). Does writing handedness affect neural representation of symbolic number? An fMRI adaptation study. *Cortex*, *121*, 27–43. https://doi.org/10.1016/j.cortex.2019.07.017

Goffin, C., Vogel, S. E., Slipenkyj, M., & Ansari, D. (2020). A comes before B, like 1 comes before 2. Is the parietal cortex sensitive to ordinal relationships in both numbers and letters? An fMRI-adaptation study. *Human Brain Mapping*, *41*(6), 1591–1610. https://doi.org/10.1002/hbm.24897

Grill-Spector, K., & Weiner, K. S. (2014). The functional architecture of the ventral temporal cortex and its role in categorization. *Nature Reviews Neuroscience*, *15*(8), 536–548. https://doi.org/10.1038/nrn3747

Grotheer, M., Ambrus, G. G., & Kovács, G. (2016). Causal evidence of the involvement of the number form area in the visual detection of numbers and letters. *NeuroImage*, *132*, 314–319. https://doi.org/10.1016/j.neuroimage.2016.02.069

Grotheer, M., Herrmann, K.-H., & Kovacs, G. (2016). Neuroimaging Evidence of a Bilateral Representation for Visually Presented Numbers. *Journal of Neuroscience*, *36*(1), 88–97. https://doi.org/10.1523/JNEUROSCI.2129-15.2016

Grotheer, M., Jeska, B., & Grill-Spector, K. (2018). A preference for mathematical processing outweighs the selectivity for Arabic numbers in the inferior temporal gyrus. *NeuroImage*, *175*(November 2017), 188–200. https://doi.org/10.1016/j.neuroimage.2018.03.064

Gullick, M. M., & Temple, E. (2011). Are historic years understood as numbers or events? An fMRI

study of numbers with semantic associations. *Brain and Cognition*, *77*(3), 356–364. https://doi.org/10.1016/j.bandc.2011.09.004

Gwilliams, L., & King, J.-R. (2020). Recurrent processes support a cascade of hierarchical decisions. *ELife*, *9*, 1–20. https://doi.org/10.7554/eLife.56603

Hannagan, T., Amedi, A., Cohen, L., Dehaene-Lambertz, G., & Dehaene, S. (2015). Origins of the specialization for letters and numbers in ventral occipitotemporal cortex. *Trends in Cognitive Sciences*, *19*(7), 374–382. https://doi.org/10.1016/j.tics.2015.05.006

Holloway, I. D., Battista, C., Vogel, S. E., & Ansari, D. (2013). Semantic and Perceptual Processing of Number Symbols: Evidence from a Cross-linguistic fMRI Adaptation Study. *Journal of Cognitive Neuroscience*, *25*(3), 388–400. https://doi.org/10.1162/jocn_a_00323

Holloway, I. D., Price, G. R., & Ansari, D. (2010). Common and segregated neural pathways for the processing of symbolic and nonsymbolic numerical magnitude: An fMRI study. *NeuroImage*, *49*(1), 1006–1017. https://doi.org/http://dx.doi.org/10.1016/j.neuroimage.2009.07.071

Hubbard, E. M., Piazza, M., Pinel, P., & Dehaene, S. (2005). Interactions between number and space in parietal cortex. *Nature Reviews Neuroscience*, *6*(6), 435–448. https://doi.org/10.1038/nrn1684

Hull, A. J. (1973). A letter-digit metric of auditory confusions. *British Journal of Psychology*, *64*(4), 579–585.

Hyde, D. C. (2021). The emergence of a brain network for numerical thinking. *Child Development Perspectives*.

Hyde, D. C., Boas, D. A., Blair, C., & Carey, S. (2010). Near-infrared spectroscopy shows right parietal specialization for number in pre-verbal infants. *NeuroImage*, *53*(2), 647–652. https://doi.org/10.1016/j.neuroimage.2010.06.030

Jansen, A., Menke, R., Sommer, J., Förster, A. F., Bruchmann, S., Hempleman, J., Weber, B., & Knecht, S. (2006). The assessment of hemispheric lateralization in functional MRI-Robustness and reproducibility. *NeuroImage*, *33*(1), 204–217. https://doi.org/10.1016/j.neuroimage.2006.06.019

JASP Team. (2020). *JASP (Version 0.14.1) [Computer software]*. https://jasp-stats.org/

Jimura, K., & Poldrack, R. A. (2012). Analyses of regional-average activation and multivoxel pattern information tell complementary stories. *Neuropsychologia*, *50*(4), 544–552. https://doi.org/10.1016/j.neuropsychologia.2011.11.007

Kay, K. N., & Yeatman, J. D. (2017). Bottom-up and top-down computations in word- and face-selective cortex. *ELife*, *6*, 1–29. https://doi.org/10.7554/elife.22341

Kimura, D. (1966). Dual functional asymmetry of the brain in visual perception. *Neuropsychologia*, *4*(3), 275–285. https://doi.org/10.1016/0028-3932(66)90033-9

Knops, A., Nuerk, H.-C., Fimm, B., Vohn, R., & Willmes, K. (2006). A special role for numbers in working memory? An fMRI study. *NeuroImage*, *29*(1), 1–14. https://doi.org/10.1016/j.neuroimage.2005.07.009

Knops, A., Nuerk, H.-C., Sparing, R., Foltys, H., & Willmes, K. (2006). On the functional role of human parietal cortex in number processing: How gender mediates the impact of a 'virtual lesion' induced by rTMS. *Neuropsychologia*, *44*(12), 2270–2283. https://doi.org/http://dx.doi.org/10.1016/j.neuropsychologia.2006.05.011

Kojouharova, P., & Krajcsi, A. (2019). Two components of the Indo-Arabic numerical size effect. *Acta Psychologica*, *192*(June 2018), 163–171. https://doi.org/10.1016/j.actpsy.2018.11.009

Kosslyn, S. M., Koenig, O., Barrett, A., Cave, C. B., & et al. (1989). Evidence for two types of spatial representations: Hemispheric specialization for categorical and coordinate relations. *Journal of Experimental Psychology: Human Perception and Performance*, *15*(4), 723–735.

https://doi.org/10.1037//0096-1523.15.4.723
Krajcsi, A., Lengyel, G., & Kojouharova, P. (2016). The source of the symbolic numerical distance and size effects. *Frontiers in Psychology*, *7*(NOV), 1–16. https://doi.org/10.3389/fpsyg.2016.01795
Kriegeskorte, N., Mur, M., & Bandettini, P. A. (2008). Representational similarity analysis - connecting the branches of systems neuroscience. *Frontiers in Systems Neuroscience*, *2*(November), 4. https://doi.org/10.3389/neuro.06.004.2008
Lancaster, J. L., Tordesillas-Gutiérrez, D., Martinez, M., Salinas, F., Evans, A., Zilles, K., Mazziotta, J. C., & Fox, P. T. (2007). Bias between MNI and talairach coordinates analyzed using the ICBM-152 brain template. *Human Brain Mapping*, *28*(11), 1194–1205. https://doi.org/10.1002/hbm.20345
Leys, C., Delacre, M., Mora, Y. L., Lakens, D., & Ley, C. (2019). How to classify, detect, and manage univariate and multivariate outliers, with emphasis on pre-registration. *International Review of Social Psychology*, *32*(1), 1–10. https://doi.org/10.5334/irsp.289
Leys, C., Klein, O., Dominicy, Y., & Ley, C. (2018). Detecting multivariate outliers: Use a robust variant of the Mahalanobis distance. *Journal of Experimental Social Psychology*, *74*(March 2017), 150–156. https://doi.org/10.1016/j.jesp.2017.09.011
Lochy, A., & Schiltz, C. (2019). Lateralized Neural Responses to Letters and Digits in First Graders. *Child Development*, *90*(6), 1866–1874. https://doi.org/10.1111/cdev.13337
Lyons, I. M., & Beilock, S. L. (2018). Characterizing the neural coding of symbolic quantities. *NeuroImage*, *178*(September), 503–518. https://doi.org/10.1016/j.neuroimage.2018.05.062
McCloskey, M., & Schubert, T. (2014). Shared versus separate processes for letter and digit identification. *Cognitive Neuropsychology*, *31*(5–6), 437–460. https://doi.org/10.1080/02643294.2013.869202
McGugin, R. W., Van Gulick, A. E., Tamber-Rosenau, B. J., Ross, D. A., & Gauthier, I. (2015). Expertise effects in face-selective areas are robust to clutter and diverted attention, but not to competition. *Cerebral Cortex*, *25*(9), 2610–2622. https://doi.org/10.1093/cercor/bhu060
Miozzo, M., & Caramazza, A. (1998). Varieties of pure alexia: The case of failure to access graphemic representations. *Cognitive Neuropsychology*, *15*(1–2), 203–238. https://doi.org/10.1080/026432998381267
Misaki, M., Kim, Y., Bandettini, P. A., & Kriegeskorte, N. (2010). Comparison of multivariate classifiers and response normalizations for pattern-information fMRI. *NeuroImage*, *53*(1), 103–118. https://doi.org/10.1016/j.neuroimage.2010.05.051
Nemmi, F., Schel, M. A., & Klingberg, T. (2018). Connectivity of the Human Number Form Area Reveals Development of a Cortical Network for Mathematics. *Frontiers in Human Neuroscience*, *12*(November), 1–15. https://doi.org/10.3389/fnhum.2018.00465
Nieto-Castañón, A., & Fedorenko, E. (2012). Subject-specific functional localizers increase sensitivity and functional resolution of multi-subject analyses. *NeuroImage*, *63*(3), 1646–1669. https://doi.org/10.1016/j.neuroimage.2012.06.065
Nieuwenhuis, S., Forstmann, B. U., & Wagenmakers, E. J. (2011). Erroneous analyses of interactions in neuroscience: A problem of significance. *Nature Neuroscience*, *14*(9), 1105–1107. https://doi.org/10.1038/nn.2886
Nili, H., Walther, A., Alink, A., & Kriegeskorte, N. (2020). Inferring exemplar discriminability in brain representations. *PLOS ONE*, *15*(6), e0232551. https://doi.org/10.1371/journal.pone.0232551
Nili, H., Wingfield, C., Walther, A., Su, L., Marslen-Wilson, W., & Kriegeskorte, N. (2014). A

Toolbox for Representational Similarity Analysis. *PLoS Computational Biology*, *10*(4), e1003553. https://doi.org/10.1371/journal.pcbi.1003553

Notebaert, K., & Reynvoet, B. (2009). Different magnitude representations in left and right hemisphere: Evidence from the visual half field technique. *Laterality*, *14*(3), 228–245. https://doi.org/10.1080/13576500802349650

Park, J., Chiang, C., Brannon, E. M., & Woldorff, M. G. (2014). Experience-dependent Hemispheric Specialization of Letters and Numbers Is Revealed in Early Visual Processing. *Journal of Cognitive Neuroscience*, *26*(10), 2239–2249. https://doi.org/10.1162/jocn_a_00621

Park, J., Hebrank, A., Polk, T. A., & Park, D. C. (2012). Neural Dissociation of Number from Letter Recognition and Its Relationship to Parietal Numerical Processing. *Journal of Cognitive Neuroscience*, *24*(1), 39–50. https://doi.org/10.1162/jocn_a_00085

Park, J., van den Berg, B., Chiang, C., Woldorff, M. G., & Brannon, E. M. (2018). Developmental trajectory of neural specialization for letter and number visual processing. *Developmental Science*, *21*(3), 1–14. https://doi.org/10.1111/desc.12578

Piazza, M., Mechelli, A., Price, C. J., & Butterworth, B. (2006). Exact and approximate judgements of visual and auditory numerosity: An fMRI study. *Brain Research*, *1106*(1), 177–188. https://doi.org/10.1016/j.brainres.2006.05.104

Piazza, M., Pinel, P., Le Bihan, D., & Dehaene, S. (2007). A Magnitude Code Common to Numerosities and Number Symbols in Human Intraparietal Cortex. *Neuron*, *53*(2), 293–305. https://doi.org/10.1016/j.neuron.2006.11.022

Pinel, P., & Dehaene, S. (2010). Beyond Hemispheric Dominance: Brain Regions Underlying the Joint Lateralization of Language and Arithmetic to the Left Hemisphere. *Journal of Cognitive Neuroscience*, *22*(1), 48–66. https://doi.org/10.1162/jocn.2009.21184

Pinel, P., Dehaene, S., Rivière, D., & LeBihan, D. (2001). Modulation of parietal activation by semantic distance in a number comparison task. *NeuroImage*, *14*(5), 1013–1026. https://doi.org/10.1006/nimg.2001.0913

Pinel, P., Le Clec'H, G., van de Moortele, P.-F. F., Naccache, L., Le Bihan, D., Dehaene, S., Le Clec'H, G., van de Moortele, P.-F. F., Naccache, L., Le Bihan, D., & Dehaene, S. (1999). Event-related fMRI analysis of the cerebral circuit for number comparison. *NeuroReport*, *10*(7), 1473–1479. https://doi.org/10.1097/00001756-199905140-00015

Pinheiro-Chagas, P., Daitch, A., Parvizi, J., & Dehaene, S. (2018). Brain Mechanisms of Arithmetic: A Crucial Role for Ventral Temporal Cortex. *Journal of Cognitive Neuroscience*, *30*(12), 1757–1772. https://doi.org/10.1162/jocn_a_01319

Pollack, C., & Price, G. R. (2019). Neurocognitive mechanisms of digit processing and their relationship with mathematics competence. *NeuroImage*, *185*, 245–254. https://doi.org/10.1016/j.neuroimage.2018.10.047

Price, C. J., & Devlin, J. T. (2011). The Interactive Account of ventral occipitotemporal contributions to reading. *Trends in Cognitive Sciences*, *15*(6), 246–253. https://doi.org/10.1016/j.tics.2011.04.001

Ratinckx, E., Nuerk, H.-C., van Dijck, J.-P., & Willmes, K. (2006). Effects of Interhemispheric Communication on Two-Digit Arabic Number Processing. *Cortex*, *42*(8), 1128–1137. https://doi.org/http://dx.doi.org/10.1016/S0010-9452(08)70225-9

Richler, J. J., Tomarken, A. J., Sunday, M. A., Vickery, T. J., Ryan, K. F., Floyd, R. J., Sheinberg, D., Wong, A. C. N., & Gauthier, I. (2019). Individual differences in object recognition. *Psychological Review*, *126*(2), 226–251. https://doi.org/10.1037/rev0000129

Richler, J. J., Wilmer, J. B., & Gauthier, I. (2017). General object recognition is specific: Evidence

from novel and familiar objects. *Cognition*, *166*, 42–55. https://doi.org/10.1016/j.cognition.2017.05.019

Rousselet, G. A., & Pernet, C. R. (2012). Improving standards in brain-behavior correlation analyses. *Frontiers in Human Neuroscience*, *6*(May), 119. https://doi.org/10.3389/fnhum.2012.00119

Roux, F. E., Lubrano, V., Lauwers-Cances, V., Giussani, C., & Demonet, J.-F. (2008). Cortical areas involved in Arabic number reading. *Neurology*, *70*(3), 210–217. https://doi.org/10.1212/01.wnl.0000297194.14452.a0

Sandrini, M., Rossini, P. M., & Miniussi, C. (2004). The differential involvement of inferior parietal lobule in number comparison: a rTMS study. *Neuropsychologia*, *42*(14), 1902–1909. https://doi.org/http://dx.doi.org/10.1016/j.neuropsychologia.2004.05.005

Schubert, T. M. (2017). Why are digits easier to identify than letters? *Neuropsychologia*, *95*(December 2016), 136–155. https://doi.org/10.1016/j.neuropsychologia.2016.12.016

Seghier, M. L. (2008). Laterality index in functional MRI: methodological issues. *Magnetic Resonance Imaging*, *26*(5), 594–601. https://doi.org/10.1016/j.mri.2007.10.010

Seghier, M. L. (2019). Categorical laterality indices in fMRI: a parallel with classic similarity indices. *Brain Structure and Function*, *224*(3), 1377–1383. https://doi.org/10.1007/s00429-019-01833-9

Sergent, J. (1990). Furtive incursions into bicameral minds. *Brain*, *113*(2), 537–568. https://doi.org/10.1093/brain/113.2.537

Seymour, S. E., Reuter-lorenz, P. A., & Gazzaniga, M. S. (1994). The disconnection syndrome: Basic findings reaffirmed. *Brain*, *117*(1), 105–115. https://doi.org/10.1093/brain/117.1.105

Shum, J., Hermes, D., Foster, B. L., Dastjerdi, M., Rangarajan, V., Winawer, J., Miller, K. J., & Parvizi, J. (2013). A brain area for visual numerals. *The Journal of Neuroscience*, *33*(16), 6709–6715. https://doi.org/10.1523/JNEUROSCI.4558-12.2013

Skagenholt, M., Träff, U., Västfjäll, D., & Skagerlund, K. (2018). Examining the Triple Code Model in numerical cognition: An fMRI study. *PLOS ONE*, *13*(6), e0199247. https://doi.org/10.1371/journal.pone.0199247

Taylor, D. A. (1978). Identification and categorization of letters and digits. *Journal of Experimental Psychology: Human Perception and Performance*, *4*(3), 423–439. https://doi.org/10.1037/0096-1523.4.3.423

Teng, E. L., & Sperry, R. W. (1973). Interhemispheric interaction during simultaneous bilateral presentation of letters or digits in commissurotomized patients. *Neuropsychologia*, *11*(2), 131–140. https://doi.org/10.1016/0028-3932(73)90001-8

Verguts, T., & Fias, W. (2004). Representation of Number in Animals and Humans: A Neural Model. *Journal of Cognitive Neuroscience*, *16*(9), 1493–1504. https://doi.org/10.1162/0898929042568497

Vogel, J. J., Bowers, C. A., & Vogel, D. S. (2003). Cerebral lateralization of spatial abilities: A meta-analysis. *Brain and Cognition*, *52*(2), 197–204. https://doi.org/10.1016/S0278-2626(03)00056-3

Vogel, S. E., Goffin, C., & Ansari, D. (2015). Developmental specialization of the left parietal cortex for the semantic representation of Arabic numerals: An fMR-adaptation study. *Developmental Cognitive Neuroscience*, *12*(1), 61–73. https://doi.org/10.1016/j.dcn.2014.12.001

Vogel, S. E., Goffin, C., Bohnenberger, J., Koschutnig, K., Reishofer, G., Grabner, R. H., & Ansari, D. (2017). The left intraparietal sulcus adapts to symbolic number in both the visual and auditory modalities: Evidence from fMRI. *NeuroImage*, *153*(June), 16–27. https://doi.org/10.1016/j.neuroimage.2017.03.048

Wilcox, R. R. (2004). Inferences based on a skipped correlation coefficient. *Journal of Applied Statistics*, *31*(2), 131–143. https://doi.org/10.1080/0266476032000148821

Wilkey, E. D., Conrad, B. N., Yeo, D. J., & Price, G. R. (2020). Shared Numerosity Representations Across Formats and Tasks Revealed with 7 Tesla fMRI: Decoding, Generalization, and Individual Differences in Behavior. *Cerebral Cortex Communications*, *1*(1), 1–19. https://doi.org/10.1093/texcom/tgaa038

Willems, R. M., Der Haegen, L. Van, Fisher, S. E., & Francks, C. (2014). On the other hand: Including left-handers in cognitive neuroscience and neurogenetics. *Nature Reviews Neuroscience*, *15*(3), 193–201. https://doi.org/10.1038/nrn3679

Woodcock, R. W., McGrew, K. S., & Mather, N. (2001). *Woodcock-Johnson III Tests of Achievement*. Riverside.

Yeo, D. J., Pollack, C., Merkley, R., Ansari, D., & Price, G. R. (2020). The "Inferior Temporal Numeral Area" distinguishes numerals from other character categories during passive viewing: A representational similarity analysis. *NeuroImage*, *214*, 116716. https://doi.org/10.1016/j.neuroimage.2020.116716

Yeo, D. J., Wilkey, E. D., & Price, G. R. (2017). The search for the number form area: A functional neuroimaging meta-analysis. *Neuroscience & Biobehavioral Reviews*, *78*, 145–160. https://doi.org/10.1016/j.neubiorev.2017.04.027